Irradiation Records, Cosmic-Ray Exposure Ages, and Transfer Times of Meteorites

O. Eugster
University of Bern

G. F. Herzog
Rutgers University

K. Marti
University of California, San Diego

M. W. Caffee
Purdue University

During the 4.56-G.y. history of the solar system, every meteorite experienced at least one exposure to cosmic rays as a meter-sized meteoroid. The cosmic-ray exposure (CRE) age of a meteorite measures the integral time of exposure to galactic cosmic rays (GCRs). A fraction of meteoritic material was also irradiated by cosmic rays before ejection from kilometer-sized parent bodies (pre-irradiation); studies of pre-irradiation effects yield information about surface processes on planetary objects. In this review we discuss some methods of calculation for CRE ages of meteorites and present CRE age histograms for asteroidal, martian, and lunar meteorites. Compositional, formation-age, and CRE records indicate that probably the ~18,000 meteorites in our collections come from about 100 different asteroids. Stone meteorites exhibit CRE ages ≤120 m.y., while those of iron meteorites are generally, but not always, longer (up to 1500 m.y.); these CRE ages also show evidence for long-term GCR flux variations in the solar neighborhood. The CRE age differences of the various classes either signal different source regions, variability in the size of the Yarkovsky effect, or different resistance against crushing. Rocks blasted off the Moon and Mars by asteroidal or cometary impacts represent surface areas unlikely to be sampled by manned or automated missions; their CRE ages indicate that they come from some eight different sites on the Moon and also on Mars.

1. INTRODUCTION

The apparent emptiness of the interplanetary space belies its complex nature. The interplanetary medium is populated by a variety of energetic particles originating from both within and outside our solar system. Earth-based ionization measurements first established the presence of galactic cosmic rays (GCRs) and energetic solar-flare particles in 1912 and 1942 respectively (cf. *Pomerantz and Duggal,* 1974). Based on the observation of comet plasma tails, *Biermann* (1951, 1953) deduced the presence of solar-wind (SW) particles in the interplanetary medium. Since then instruments on satellites have measured the primary particle fluxes directly, along with their energy spectra and elemental and isotopic abundances.

The goal of this review is to present some characteristics of the energetic particle environment during the past 0.03–1500 m.y. as inferred from the effects of particle irradiation on meteorites and lunar surface materials. Toward that end we will discuss the basic principles of nuclide production in meteorites, the calculation of exposure times or cosmic-ray exposure (CRE) ages, and the statistical distributions of these ages. We will show that the CRE ages have implications for several interrelated questions. From how many different parent bodies do meteorites come? What was their pre-atmospheric size? How well do meteorites represent the population of the asteroid belt? How many collisions on their parent bodies have created the known meteorites of each type? Is there a time variation in the cosmic-ray (CR) flux? What factors control the CRE age of a meteorite and how do meteoroid (the immediate meter-sized precursor of meteorites) orbits evolve through time?

In this review we summarize the exposure histories of asteroidal, martian, and lunar meteorites. This field of science experienced remarkable development during the past 50 years and some comprehensive reviews were published (e.g., *Anders,* 1964; *Lal,* 1972; *Reedy et al.,* 1983; *Caffee et al.,* 1988; *Vogt et al.,* 1990; *Marti and Graf,* 1992; *Wieler and Graf,* 2001; *Wieler,* 2002a; *Herzog,* 2003; *Eugster,* 2003). In this review we will not be concerned with CR interactions with the lunar surface or the surface exposure ages of lunar rocks and soils from the Apollo and Luna missions; we refer the interested reader to the reviews by *Vogt et al.* (1990) and *Eugster* (2003). We will also not dis-

cuss the ways that trapping of solar particles modifies noble gas concentrations in meteorites. *Wieler et al.* (2006) treat this subject.

The energetic particles found in our solar system can be divided into three classes: SW particles, solar energetic particles, and GCRs. Here we mainly focus on the GCR effects in meteorites. For a detailed discussion of the interactions of solar particles we refer to the reviews by *Caffee et al.* (1988) and *Wieler* (2002b).

1.1. Nature of Galactic Cosmic Rays

Galactic cosmic rays, the most energetic particles in the interplanetary medium, originate from outside our solar system. The omnidirectional flux of the GCR nuclei at 1 AU is about 3 nuclei cm^{-2} s^{-1} for particles having kinetic energy >1 GeV/nucleon. Their energy spectrum obeys a power law in energy (Fig. 1). Above ~10 GeV, the number of particles is proportional to $E^{-2.65}$, where E is the particle energy. As noted above, solar modulation influences the number of GCR nuclei penetrating the solar system, this effect being most pronounced for the low-energy (<1 GeV/nucleon) component (cf. *Castagnoli and Lal,* 1980).

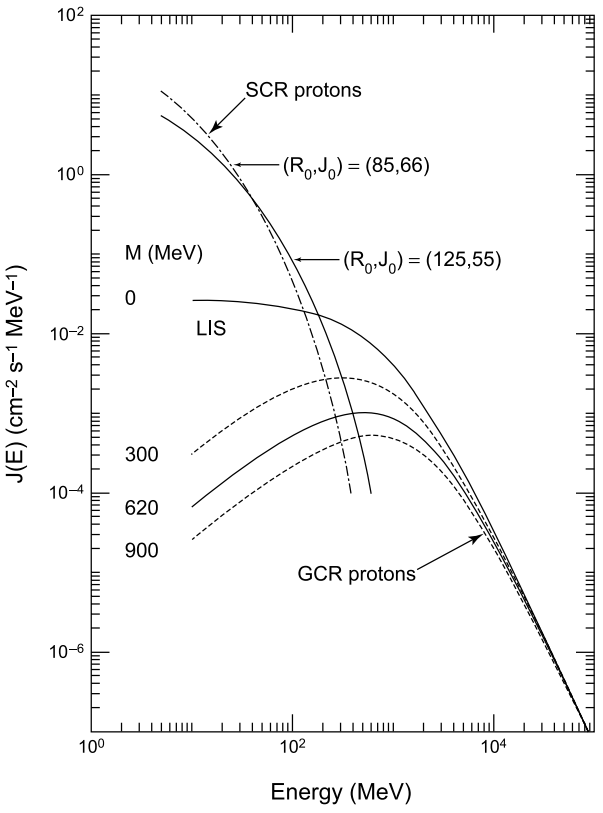

Fig. 1. Spectra of solar (SCR) and galactic (GCR) cosmic-ray protons at 1 AU. The modulation parameter, M, is shown vs. proton energy. GCR spectra are plotted for times of an active (M = 900 MeV) and a quiet (M = 300 MeV) Sun, as well as for the average GCR spectrum during the last 10 m.y. and for the local interstellar spectrum (LIS, M = 0). For original data and details see *Michel et al.* (1996).

Observed elemental abundances of GCRs are similar to solar system abundances. The similarity suggests that CRs and the nuclei in the Sun were synthesized by similar processes. The high energy of the cosmic radiation links it to shock acceleration mechanisms in supernovae environments (*Axford,* 1981; *Lingenfelter et al.,* 2000). Propagation through the interstellar medium results in the production of the light elements Li, Be, and B via nuclear "spallation" interactions, causing them to be overabundant relative to solar system values.

The CR Isotope Spectrometer (*Binns et al.,* 2001) can measure isotopic ratios of several elements in GCRs. The data of these authors support models where GCRs preferentially are from dust or gas of Wolf Rayet stars or supernovae from the central region of the galaxy. The isotopic composition of these elements usually agrees with the solar system abundances. An outstanding exception to this is the $^{20}Ne/^{22}Ne$ ratio. In galactic CRs, ^{22}Ne is enriched relative to either SW-implanted Ne or the trapped Ne component observed in many meteorites (*Binns et al.,* 2001). This observation is interesting in light of the occurrence of essentially pure ^{22}Ne (Ne-E) in several meteorites (*Eberhardt,* 1974; *Eberhardt et al.,* 1979).

1.2. Products of Interactions of Energetic Particles with Extraterrestrial Matter

Energetic particles interact with solid matter in a variety of ways. In order to decipher the exposure history of a meteorite it is necessary to understand these interactions. The dominant modes of interaction are determined by the energy and mass of the incident particle. At the low end of the energy spectrum are the SW nuclei. Their energies are so low that they simply stop; in the language of specialists, they are referred to as "implanted." At the other end of the energy spectrum are mainly protons and α-particles in the GCRs. These particles possess enough energy to induce nuclear reactions in material.

1.2.1. Direct implantation. Particles in the SW with low energy (~1 keV/nucleon) only penetrate solids to depths of ~50 nm, although subsequent diffusion of the implanted nuclei within the solid may result in an altered depth distribution. In stopping, the low-energy SW ions also cause radiation damage on the surface of solids. Because of the high flux of SW ions, mineral grains exposed to the SW can become saturated (that is, reach a limiting equilibrium concentration), especially for lighter elements. For instance, at 1 AU, 200 year is sufficient to reach He saturation. Not surprisingly, many lunar grains are saturated with SW-implanted He.

1.2.2. Energy loss and lattice damage. Energetic very heavy particles with Z > 20 (VH nuclei) slow down, near the end of their range. In many silicate materials they create permanent "latent" damage trails. These trails are observed directly by transmission electron microscopy or are chemically etched and enlarged to produce a conical hole that is visible by optical microscopy. These damage trails

or etch holes are termed nuclear tracks. [For a review of this technique see *Fleischer et al.* (1975).] The tracks in silicate grains are produced by nuclei from both solar cosmic ray (SCRs) and GCRs. These two sources of tracks can be distinguished from each other. Galactic-cosmic-ray VH nuclei can penetrate solid matter to depths of several centimeters, whereas SF-VH nuclei have a range of <0.1 cm in solid matter. In this shorter range, SCR-produced tracks are far more prevalent than GCR-produced tracks, as shown in Fig. 1. Thus SCR-produced tracks are usually characterized by high track densities and track-density gradients, reflecting the steeply falling energy spectra of the SCR nuclei. The relationship between the track density, ρ, and the depth, x, can be described by the power law

$$\rho\ (x) \text{ proportional to } x^{\eta} \qquad (1)$$

where η, the power-law exponent, is the slope of the semilogarithmic track-density profile and depends on the size of the object (in space). The relationship between the energy, E, of the incident particle and its range S is given by

$$S \text{ proportional to } E^{\beta} \qquad (2)$$

where β can be determined in experiments at particle accelerators. Since tracks are produced at the end of a particle's range, and the track density as a function of depth x is proportional to the number of track-forming particles stopping at depth x, we have

$$\rho \text{ proportional to } \left(\frac{dN}{dS}\right)_x = \left(\frac{dN}{dE} \times \frac{dE}{dS}\right)_x \qquad (3)$$

where the decrease in kinetic energy, E, is expressed by

$$\frac{dN}{dE} = \text{constant} \times E^{-\gamma} \qquad (4)$$

The power law exponent, γ, defines the spectral hardness, which, for regions below the surface, also depends on the size of the irradiated object. The term dE/dS can be derived from equation (2). Substituting these derivatives into equation (3) and equating it to equation (1) produces

$$\eta = (1/\beta)(\gamma + \beta - 1) \qquad (5)$$

This equation describes the dependence of the spectral shape of the track-forming heavy nuclei on the power-law exponent, η, of the incident primary nuclei (*Fleischer et al.,* 1967, 1975; *Bhattacharya et al.,* 1973).

1.2.3. Nuclear reactions. The energetic, charged particles that bombard a meteoroid can have any one of three fates: (1) the particles can escape; (2) they can stop without causing nuclear reactions; or (3) they can enter into a nuclear reaction. The relative probabilities depend on initial particle energy and atomic number, and on meteoroid size and composition. At low energies, stopping without reaction is the most likely outcome. The particle energy at which the probability of loss by nuclear reaction (3) is equal to the probability of survival, the crossover point, is ~300 MeV/nucleon. Since the ionization loss is proportional to Z^2, the crossover energy increases for high Z particles.

To induce a nuclear reaction, the bombarding particles must have at least several megaelectron volts of energy. Of the more energetic particles in the solar system, protons and α-particles from the Sun (SCRs) as well as GCRs produce nuclear reactions. Solar-cosmic-ray primaries typically produce reactions with small mass losses, such as $^{56}Fe(p,n)^{56}Co$, where an energetic proton reacts with a ^{56}Fe target nucleus to produce ^{56}Co and a (secondary) neutron. Primary and secondary GCRs have a broad energy spectrum and accordingly induce a large variety of high- and low-energy nuclear reactions. Galactic-cosmic-ray primaries account for most high-energy reactions where nuclear spallation reactions dominate. The secondary GCR particle cascade, especially the neutrons, account for lower-energy reactions (<100 MeV). At the low-energy end of nuclear reactions, epithermal and thermal neutron reactions, such as $^{157}Gd(n,\gamma)^{58}Gd$, produce nuclides by neutron capture (see below).

Nuclear reactions in meteorites are quite rare. Over a period of typical CRE ages of meteorites (~10 m.y.), only about one in every 10^8 nuclei undergoes a nuclear transformation. The "cosmogenic" nuclides are products of GCR- or SCR-produced nuclides, either radioactive or stable nuclides of exceedingly low initial abundance, such as noble gases. Table 1 shows a compilation of the measured cosmogenic nuclides in meteorites.

2. SHIELDING AND PRE-ATMOSPHERIC SIZE

The size of a meteoroid in space cannot be determined directly from the recovered mass of a meteorite because of the unknown degrees of ablation and fragmentation. Size must therefore be inferred from various experimental measurements and model calculations. Because of the imprecision of these models and for convenience, meteoriticists usually assume that meteoroids are spherical and express their "sizes" as radii. The most common units for the radii are either centimeters or grams per square centimeters, where unit (g/cm^2) = radius (cm) × density (g/cm^3). The use of units of grams per square centimeters, which borrows from the practice of nuclear physicists, has the advantage of correlating better with the number of atoms available for nuclear reactions in a meteoroid than does the radius expressed in centimeters.

As we will see below, the rates of nuclear reactions in a spherical meteoroid are strongly influenced by the original "depth" of the sample analyzed in the meteoroid, which is to say the shortest distance from the sample to the pre-atmospheric surface. In a spherical meteoroid, but not necessarily in real ones, the "depth" is a well-defined quantity.

TABLE 1. Cosmogenic nuclides measured in meteorites.

Nuclide	Half-Life (yr)	Main Targets
^{3}H	12.26	O, Mg, Si, Fe
^{3}He, ^{4}He	S*	O, Mg, Si, Fe
^{10}Be	1.51×10^{6}	O, Mg, Si, Fe
^{14}C	5730	O, Mg, Si, Fe
^{20}Ne, ^{21}Ne, ^{22}Ne	S	Mg, Al, Si, Fe
^{22}Na	2.6	Mg, Al, Si, Fe
^{26}Al	7.17×10^{5}	Si, Al, Fe
^{36}Ar, ^{38}Ar	S	Fe, Ca, K
^{36}Cl	3.01×10^{5}	Fe, Ca, K
^{37}Ar	35 d	Fe, Ca, K
^{39}Ar	269	Fe, Ca, K
^{40}K	1.251×10^{9}	Fe, Ni
^{39}K, ^{41}K	S	Fe, Ni
^{41}Ca	1.034×10^{5}	Ca, Fe
^{53}Mn	3.74×10^{6}	Fe, Ni
^{54}Mn	312 d	Fe, Ni
^{59}Ni	7.6×10^{4}	Ni
^{60}Co	5.27	Co, Ni
^{81}Kr	2.29×10^{5}	Rb, Sr, Y, Zr
^{78}Kr, ^{80}Kr, ^{82}Kr, ^{83}Kr	S	Rb, Sr, Y, Zr
^{129}I	1.57×10^{7}	Te, Ba, La, Ce
$^{124–132}$Xe	S	Te, Ba, La, Ce, (I)
^{150}Sm	S	Sm
^{156}Gd, ^{158}Gd	S	Gd

*S denotes that the nuclide is stable.

Other observed nuclides (few measurements): ^{7}Be, ^{44}Ti, ^{46}Sc, ^{55}Fe, ^{56}Co, and ^{60}Fe.

As mentioned above, secondary neutrons produced by CRs induce "low-energy" nuclear reactions. These neutrons are by custom very roughly divided into three groups according to their energy: >1 MeV, 0.1–300 eV (epithermal), and <0.1 eV (thermal). In large meteoroids of radius >200 g cm^{-2} the flux of thermal and epithermal neutrons peaks at shielding depths of 100–300 g cm^{-2} (cf. *Eberhardt et al.,* 1963; *Lingenfelter et al.,* 1972; *Spergel et al.,* 1986). The neutron flux within a meteoroid is thus a function of its size and of the shielding depth of the investigated sample within the meteoroid. Epithermal and thermal neutrons especially engage in what are called neutron-capture reactions that give rise to distinct and readily identifiable products. We show below that shielding depths and pre-atmospheric radii are important parameters for calculating the production rates of cosmogenic nuclides. Furthermore, the determination of the pre-atmospheric size of meteorites based on neutron-produced nuclides is significant for the study of the parent-body ejection dynamics of meteoritic matter. Finally, neutron-capture species may give information about exposure histories of large shielded objects that cannot be obtained from measurements of other types (high-energy spallation) of CR irradiation products alone. Complex exposures (see below) can be revealed from the relation of species produced by neutron capture that are stable with those that have relatively short half-lives.

Table 2 gives the neutron capture reactions that have been observed in meteorites. The references indicate additional information and work in which isotopic anomalies have been observed for the first time.

The determination of sample depth and meteoroid size are closely linked. The three most reliable methods for their determination within stony meteoroids are (1) combined measurements of the cosmogenic ratio ^{22}Ne/^{21}Ne and a radionuclide, (2) measurements of the production rates of nuclides produced by thermal neutrons, and (3) nuclear tracks. The ^{22}Ne/^{21}Ne ratio taken alone is not a unique function of size and depth. As a ratio, it depends strongly on the shape of the energy spectra of the primary and secondary particles and on the number of nuclear-active particles. To obtain both size and depth one must also determine the concentration of a cosmogenic radionuclide that is more sensitive to the number of active particles. For theoretical calculations showing the relation between ^{22}Ne/^{21}Ne and depth we refer to *Leya et al.* (2000) and *Masarik et al.* (2001). The reaction ^{24}Mg(n,α)^{21}Ne dominates the production of ^{21}Ne: At average shielding corresponding to about

TABLE 2. Observed CR-produced neutron capture reactions in meteorites.

Reaction	Neutron energy	Reference
^{24}Mg(n,α)^{21}Ne	> 5 MeV	[1]
^{35}Cl(n,γ)^{36}Cl(β^-)^{36}Ar	thermal	[2]
^{40}Ca(n,p)^{40}K	~6 MeV	[3]
^{40}Ca(n,γ)^{41}Ca	thermal	[4]
^{58}Ni(n,γ)^{59}Ni	thermal	[5]
^{59}Co(n,γ)^{60}Co	thermal	[6]
^{79,81}Br(n,γ)^{80,82}Br(β^-)^{80,82}Kr	epithermal (30–300 eV)	[7]
^{127}I(n,γ)^{128}I(β^-)^{128}Xe	epithermal (30–300 eV)	[7]
^{130}Ba(n,γ)^{131}Ba(β^+)^{131}Cs(e capt.)^{131}Xe	epithermal (resonance capture)	[8, 9]
^{149}Sm(n,γ)^{150}Sm	thermal	[4]
^{157,155}Gd(n,γ)^{158,156}Gd	thermal	[10]

References: [1] *Eberhardt et al.* (1966); [2] *Spergel et al.* (1986); [3] *Burnett et al.* (1966); [4] *Bogard et al.* (1995); [5] *Schnabel et al.* (1999); [6] *Cressy* (1972); [7] *Marti et al.* (1966); [8] *Eberhardt et al.* (1971); [9] *Kaiser and Rajan* (1973); [10] *Eugster et al.* (1970).

30 g cm^{-2}, about 70% of ^{21}Ne is produced by this reaction (*Michel et al.,* 1991). Neutron production of ^{22}Ne is somewhat less important than that of ^{21}Ne although it also increases with depth up to 200 g cm^{-2}. The strength of the method based on Ne lies in the fact that the analyses of the three stable Ne isotopes alone — ^{20}Ne, ^{21}Ne, and ^{22}Ne (together with the knowledge of the target element concentrations for ^{21}Ne production) — are sufficient to derive a shielding-corrected CRE age. Therefore, the ^{21}Ne–^{22}Ne/^{21}Ne dating method is most widely applied to stone meteorites. A determination of the ^{20}Ne concentration has to be included in the analyses in order to correct for other contributions to meteoritic Ne, such as primordial Ne. All other neutron-capture reactions are less suited for the determination of the shielding corrections as they require the isotopic analysis of an additional element.

The basis for using thermal neutrons for the determination of the pre-atmospheric sizes and sample depths of meteorites was set by the pioneering work of *Eberhardt et al.* (1963). These authors calculated the production of ^{36}Cl, ^{59}Ni, and ^{60}Co by n,γ-processes in spherical chondrites as a function of the meteorite radius. *Marti et al.* (1966) showed that epithermal neutrons in the energy range 30–300 eV must be responsible for an ^{80}Kr, ^{82}Kr, and ^{128}Xe anomaly observed in large meteorites. These authors calculated for the first time pre-atmospheric sizes of meteoroids based on excesses of ^{80}Kr from the reaction ^{79}Br(n,γ)^{80}Br(β$^-$)^{80}Kr and obtained minimal pre-atmospheric masses of 220 kg and 1400 kg for the Abee and the Mezö-Maderas chondrites, respectively. The detailed procedure for the calculation of the $^{80}Kr_n$ production rate, the epithermal neutron flux, the slowing-down density, and the pre-atmospheric size is given for 19 chondrites by *Eugster et al.* (1993) and for 6 martian meteorites by *Eugster et al.* (2002a). *Bogard et al.* (1995) measured significant concentrations of ^{36}Cl, ^{36}Ar, ^{41}Ca, and ^{150}Sm/^{149}Sm excesses from the capture of thermalized neutrons in the large Chico L6 chondrite. The fluence calculated from these nuclides is about 1.2×10^{16} n cm^{-2}. Neutron fluences of 10^{15}–10^{16} n cm^{-2} were also observed for three other chondrites and two achondrites. These authors concluded that the neutron-induced nuclides were produced during CRE. The rarely measured nuclide ^{59}Ni, resulting mainly from thermalized neutron capture of ^{58}Ni, was measured by *Schnabel et al.* (1999) in meteorite fragments and spherules of the Canyon Diablo impactor. These measurements imply that the liquid precursor material for the spheroids came from depths of 1.3–1.6 m beneath the pre-atmospheric surface of the impactor. *Hidaka et al.* (2000) analyzed the Sm- and Gd-isotopic composition in eight chondrites and observed evidence for neutron-capture effects. This enabled them to calculate pre-atmospheric sizes for six L and LL chondrites.

In principle, it is also possible to deduce the pre-atmospheric size and the approximate shape of a meteorite from a study of the track-density contours, since the track density drops rapidly with depth. Mass ablation estimates for 160 meteorites range between 27% and 99% with a weighted mean ablation of 85% (*Bhandari et al.,* 1980). These authors observed a relation between the pre-atmospheric mass of a meteorite, the track-production rate, and the cosmogenic ^{22}Ne/^{21}Ne ratios for shielded samples. This empirical relation can be used to determine the pre-atmospheric masses of meteorites from measurements of track densities and Ne-isotopic abundances of a few samples from interior locations.

3. DATING METHODS

3.1. Assumptions and Equations

Given certain assumptions about the conditions of irradiation and the history of a meteorite, we can calculate for that meteorite a CRE age, T. For this purpose we need measurements of the concentrations of stable and/or radioactive cosmogenic nuclides (Table 1). The assumptions are that (1) the flux of primary cosmic rays was constant in time, (2) the flux of primary cosmic rays was constant in space, (3) the shape of the sample did not change appreciably, (4) the chemical composition of the sample did not change appreciably, (5) any cosmogenic contributions from prior periods of irradiation are known, (6) all non-cosmogenic contributions to the inventory of the nuclide of interest are known, and (7) the sample did not lose nuclides of interest except by known rates of radioactive decay.

Remarkably, many meteorites seem to satisfy this set of requirements (*Leya et al.,* 2001a; *Welten et al.,* 2001a). For those meteorites, we may write for the concentration of a stable cosmogenic nuclide

$$S = P_S T \tag{6}$$

and for the concentration R of a radioactive nuclide

$$R = P_R \lambda^{-1}(1 - e^{-\lambda T}) \tag{7}$$

where P denotes the production rate and λ the decay constant.

3.2. Cosmogenic Nuclide Production Rates

Calibrations of the production rates may not be straightforward, since the production rate depends on the position of a sample within the pre-atmospheric object, which in general is difficult to ascertain. There are several methods for determining production rates: The physical methods (semi-empirical calculations) are based on measurements of cross sections and particle spectra and extensive computer calculations (cf. *Michel et al.,* 1991, 1996). Another method is based on measurements of pairs of radioactive and stable nuclides with similar nuclear-production parameters. This method requires experimental concentration data for both nuclides. The two approaches that we now discuss in more detail are not always cleanly separated.

In order to model a particular cosmogenic-nuclide-production rate (cf. *Graf et al.,* 1990a; *Michel et al.,* 1995; *Honda et al.,* 2002) it is necessary to specify several physi-

cal parameters. The production rate of a particular nucleus, P(R,d), assumed to be independent of time, is given by the relation

$$P(R,d) = \Sigma N_j \Sigma \int \sigma_{ij}(E) F_i(E,R,d) dE \quad (8)$$

where N_j is the abundance of the j^{th} target element, $\sigma_{ij}(E)$ is the cross section at energy E for producing the nuclide from particle i reacting with target nucleus j, and $F_i(E,R,d)$ is the flux of particle i at energy E in a meteoroid of radius R and at a depth d (*Arnold et al.,*1961; *Kohmann and Bender,* 1967; *Reedy,* 1985, 1987). The basic shapes for $F_i(E,R,d)$ are fairly well known, especially for high-energy GCRs. Factors influencing $F_i(E,R,d)$ are the size, shape, and composition of a meteoroid (*Reedy,* 1985). If the radius of a meteoroid is less than the interaction length of the GCRs (~100 g/cm^2), the production rates due to the primary particles do not decrease much from surface to center. The primary particles are only part of the story, however. Galactic cosmic rays also produce secondary particles, which have important effects on production rates in all but the smallest meteorites (radii <10 cm). These effects are obvious in all stony meteorites with radii between 30 and 150 g/cm^2 where production rates actually increase with depth. The energy distribution of the particles influences the production profile. Profiles of nuclides produced by relatively low-energy SCR particles, for example, decrease sharply with depth and are essentially confined to the outermost few centimeters because the SCRs produce few or no nuclear-active secondary particles. The depth profiles of nuclides produced by higher-energy GCRs, in contrast, vary by only about 30% in small- to medium sized meteorites (R ~ 30 cm) because of the ingrowth of secondary particle fluxes. Toward the interior (depths >15 cm) of larger meteorites, fluxes of both primary and secondary particles eventually decrease, typically exponentially with a half thickness of about 40 cm in stones (*Leya et al.,* 2000).

The production rate is proportional to the (energy-dependent) cross section for the production of a particular nuclide. Whenever possible, cross sections are based on direct measurements, but many are not known and must be extrapolated from experimental data or calculated from theoretical considerations. Combining the particle fluxes (both primary and secondary) with excitation functions and target-element chemistry according to equation (8) yields the production profile for a particular nuclide. Figure 2 shows the production profile for ^{21}Ne, a low-energy reaction product, and Fig. 3 shows that for ^{3}He, produced primarily in high-energy reactions.

Experimental approaches have been employed to determine the production profiles of cosmogenic nuclides in meteorites. *Graf et al.* (1990b) measured CR-produced nuclides from high- and low-energy reactions in samples from known positions within the L5 chondrite Knyahinya (R ~ 45 cm; pre-atmospheric mass 1300–1400 kg). Simulations of the GCR bombardment of meteorites were carried out using accelerator techniques, in which thick targets were irradiated with energetic protons (*Honda,* 1962). The thick-target production profiles are then translated into production

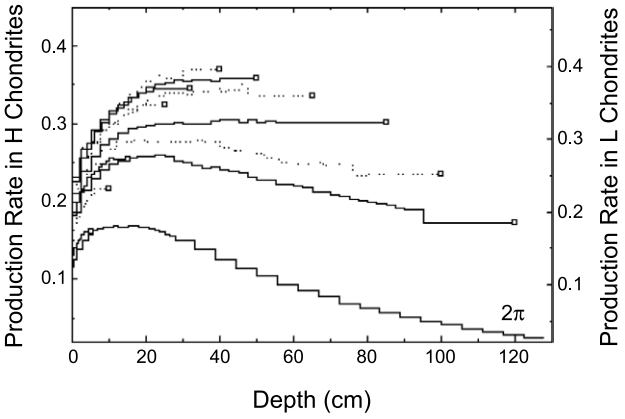

Fig. 2. Calculated production rates (in units of 10^{-8} cm^3 STP/g m.y.$^{-1}$) of ^{21}Ne for ordinary chondrites, shown for several radii vs. depth of an irradiated sample (from *Leya et al.,* 2000).

profiles for a hemispherical object (*Kohman and Bender,* 1967). This approach has been successful in predicting the production of cosmogenic nuclides in large iron meteorites.

Several thick-target experiments for the simulation of irradiations of stony and iron meteoroids with GCR protons were performed during the last two decades (e.g., *Michel et al.,* 1986; *Lüpke,* 1993; *Leya and Michel,* 1998; *Leya et al.,* 2004a). Such irradiations can be used to test and improve model calculations; for the recent examples we refer to *Michel et al.* (1991, 1995, 1996) and *Leya et al.* (2000). It is not practical to conduct simulation experiments for all the possible exposure geometries of meteorites, so theoretically derived production profiles in agreement with simulated irradiations give us confidence that the underlying theory can reliably predict production profiles for meteorites of different sizes.

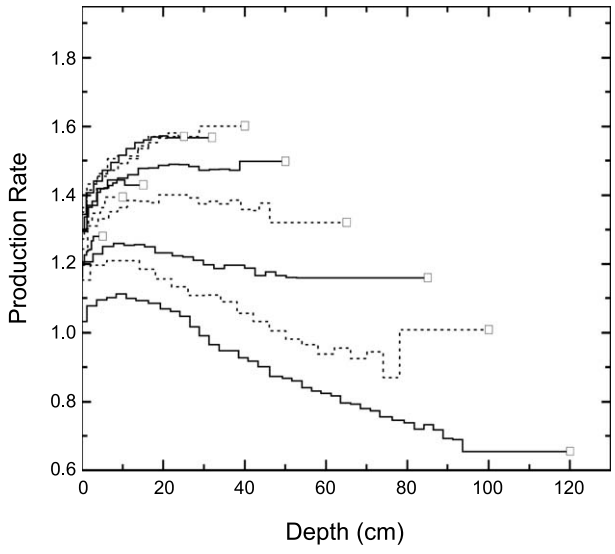

Fig. 3. Calculated production rates (in units of 10^{-8} cm^3 STP/g m.y.$^{-1}$) of ^{3}He as a function of meteorite radius and depth (*Leya et al.,* 2004a).

In the analysis of cosmogenic nuclide abundances, it is convenient to be able to estimate separately and easily the effects of composition (*Stauffer,* 1962) and shielding (*Eberhardt et al.,* 1966) on production rates without having to examine the output of detailed model calculations. So useful are the results of such formulations that since the 1960s meteoriticists have been writing production rates in the general form

$$P = f_1(\text{shielding}) \times f_2(\text{composition}) \times P_{Std} \qquad (9)$$

where P_{Std} is a normative production rate under certain "standard" conditions [cosmogenic $^{22}Ne/^{21}Ne$ ratio = 1.11; chondritic composition (see *Eugster,* 1988)]. The shielding factor, f_1, is written in terms of one or two geometry-dependent quantities such as $^{22}Ne/^{21}Ne$ ratios or radionuclide concentrations (*Graf et al.,* 1990a; *Leya et al.,* 2000). Ideally, f_1 varies systematically and uniquely with meteoroid size and sample depth.

The compositional factor, f_2, is normally written as shown in equation (10)

$$\frac{\sum_{j}^{sa} N_j P_j}{\sum_{j}^{std} N_j P_j} \qquad (10)$$

where sa stands for "sample" and std for "standard." N_j are elemental abundances (assumed uniform throughout the meteoroid) and P_j are the corresponding (nominal) production rates for each element that are taken from model calculations, but can also be obtained from meteoritic analyses (e.g., *Stauffer,* 1962). A key assumption here is that under fixed geometric irradiation conditions the values of P_j are constant and secondary particle fluxes do not depend on composition. However, equation (8) cannot be transformed into equation (9) without (falsely) assuming composition-independent secondary particle fluxes contributing to f values. For the relatively small ranges in composition found in H, L, and LL chondrites, this assumption is appropriate and equation (10) works well. On the other hand, for large differences in composition larger errors arise in the production rates based on equation (9) (*Begemann and Schultz,* 1988). *Masarik and Reedy* (1994) compared the model-production rates in mesosiderites and ordinary chondrites. For samples irradiated at an average depth of 57 g/cm^2 in objects with radii of 100 g/cm^2, they found the production rate of ^{21}Ne from Mg was 80% higher in the mesosiderites. The dependence of the nominal elemental production rates, P_j, on bulk composition is a consequence of what is called the matrix effect. Stated in general terms, the matrix effect refers to how, under fixed geometric conditions, elemental composition influences the secondary flux of nuclear particles and, through those fluxes, production rates.

Production rates may also be determined solely from analyses of meteorites. We consider P_R first. For meteorites with CRE ages long compared to the relevant half-life, $T \gg t_{1/2} = \ln(2)/\lambda$, we have $R = P_R \lambda^{-1}$. The quantity P_R varies from sample to sample as composition and shielding change. Shielding can depress P_R for a given nuclide tenfold or more in a large meteorite, but variations of less than ±30% around the average are much more typical for small- and medium-sized objects. Thus, we can apply equation (7) using an average value of P_R, obtained by averaging measurements of many meteorites with long exposure ages, and a value of R in another meteorite with an unknown age. This procedure yields a first approximation for the CRE age for objects with $T \leq 2 \times t_{1/2}$. Analogously, we can obtain relative CRE ages from equation (6) simply by comparing the measured concentrations of stable nuclides.

To obtain more precise and absolute CRE ages one must account for the effects of shielding sample by sample. The corrections for shielding are made by determining pairs of carefully selected stable and radioactive cosmogenic nuclides and forming the ratio of their concentrations. By combining equations (6) and (7), we have

$$S/R = \lambda P_s P_R^{-1} T(1 - e^{-\lambda T})^{-1} \qquad (11)$$

If similar nuclear reactions produce nuclides S and R, then we expect the ratio P_S/P_R to vary little with shielding. Thus, to calculate absolute CRE ages from equation (11), we need to determine P_S/P_R at least once, and for the most precise work, to develop an expression for P_S/P_R that has a known dependence on shielding (see below) and compensates adequately for matrix effects. Examples of reliable methods for calculating CRE ages that incorporate these requirements for stones are based on (1) $^{81}Kr/Kr$ ratios and (2) coupled analyses of ^{21}Ne and the $^{22}Ne/^{21}Ne$ ratio. This latter method is not independent because it is pegged to the $^{81}Kr/Kr$ CRE ages of groups of meteorites (see below). For iron meteorites a frequently used method is based on $^{36}Cl/^{36}Ar$ concentration ratios. These methods will be discussed below. For other methods, such as those based on other stable noble gas species and appropriate production rates, $^{10}Be/^{21}Ne$, $^{26}Al/^{21}Ne$, and $^{40}K/K$ we refer to the reviews by *Herzog* (2003) and *Wieler* (2002a).

3.3. Calculation of Cosmic-Ray Exposure Ages

3.3.1. Krypton-81/krypton-83 cosmic-ray exposure ages. The main target nuclei for the production of Kr isotopes in stony meteorites are those of the trace elements Rb, Sr, Y, and Zr. As the isotopic Kr production rate ratios depend very weakly on the relative concentrations of these elements, their concentrations must be known only for the most precise CRE ages. Adapting equation (11), we have

$$^{83}Kr/^{81}Kr = (\lambda P_{83} T)/[P_{81}(1 - e^{-\lambda T})] \qquad (12)$$

where λ is the ^{81}Kr decay constant. By measuring all Kr-isotopic ratios in one mass spectrometer run, one avoids the systematic biases that may affect the determination of CRE ages that rest on concentration measurements made with different instruments (*Marti,* 1967; *Eugster et al.,* 1967).

The production-rate ratio was originally determined from considerations of nuclear reaction systematics and nuclear cross-section measurements on the element Ag. However, it is now updated as

$$P_{81}/P_{83} = 0.92(^{80}Kr + ^{82}Kr)/(2 \times ^{83}Kr) \quad (13)$$

where the factor 0.92 is the isobaric fraction yield of ^{81}Kr determined from proton cross-section measurements on the main meteoritic target elements Rb, Sr, Y, and Zr (*Gilabert et al.,* 2002). Nuclear reactions on Br induced by low-energy secondary neutrons affect the relative production rates of ^{80}Kr and ^{82}Kr. Consequently, variations in the production-rate ratios ^{80}Kr/^{83}Kr and ^{82}Kr/^{83}Kr may often occur, thereby invalidating the use of equation (13). *Marti and Lugmair* (1971) circumvented the problem by determining P_{81}/P_{83} based on the ^{78}Kr/^{83}Kr ratio in lunar rocks. The approach also works for meteorites because low-energy neutrons do not affect the relative concentrations of either ^{78}Kr or ^{83}Kr, even in larger meteorites. For constants in equation (14) see *Eugster et al.* (2002a) and *Leya et al.* (2004b), who calculated slightly different values for chondrites

$$\frac{P_{81}}{P_{83}} = 1.174\left(\frac{^{78}Kr}{^{83}Kr}\right)_{spallogenic} + 0.354 \quad (14)$$

3.3.2. Neon-21 ages with shielding corrections based on neon-22/neon-21 ratios. *Nishiizumi et al.* (1980) and *Eugster* (1988) developed an empirical expression for the production rates of ^{21}Ne in ordinary chondrites, and *Eugster and Michel* (1995) extended this work to achondrites. *Eugster* (1988) used the ^{81}Kr/Kr CRE ages, cosmogenic ^{21}Ne contents, and ^{22}Ne/^{21}Ne ratios of a suite of ordinary chondrites and determined ^{21}Ne production rates based on ^{81}Kr/Kr CRE ages. In previous work *Eberhardt et al.* (1966) had argued that the ^{21}Ne production rate depends on the ^{22}Ne/^{21}Ne ratio according to the empirical relation

$$P^{21} = [a(^{22}Ne/^{21}Ne) + b]^{-1} \quad (15)$$

Though not rigorously defensible, this mathematical form fits the available data for many meteorites reasonably well, and yields the following equation for L chondrites, where the production rate results in units of 10^{-8} cm^3 STP/g m.y.$^{-1}$

$$P_{21} = [13.52(^{22}Ne/^{21}Ne) - 12.00]^{-1} \quad (16)$$

Minor adjustments for the other chondritic meteorites are discussed by *Eugster* (1988). However, equation (16) is not suitable for ^{22}Ne/^{21}Ne ratios less than about 1.08, i.e., for samples recovered from the interiors of larger meteoroids (*Masarik et al.,* 2001; *Leya et al.,* 2001b).

As developed by *Eugster* (1988) for ordinary chondrites, equation (16) assumes that composition dependence can be expressed by equation (9) with particular values of P_j taken from the work of *Freundel et al.* (1986) on ordinary chondrites. The matrix effect does not allow one to apply equation (16) to meteorites with compositions very different from those of ordinary chondrites. Recognizing this problem, *Eugster and Michel* (1995) recalibrated equation (16) for achondrites. *Albrecht et al.* (2000) found that on average, the equations of *Eugster and Michel* (1995) gave reliable production rates also for mesosiderites and concluded that the ^{22}Ne/^{21}Ne ratio has considerable capacity to correct for both shielding and composition. In sum, although the matrix effect can be large and is of theoretical interest, modeling calculations automatically take it into account, and standard calculations of CRE ages compensate adequately for it.

3.3.3. Chlorine-36/argon-36 cosmic-ray exposure ages. The principal target nuclei for the production of ^{36}Cl and ^{36}Ar in iron meteorites and in the metal phase of stony ones are the elements Fe and Ni (e.g., *Begemann et al.,* 1976). Once produced, ^{36}Cl decays with a half-life of 0.30 m.y. in part to ^{36}Ar. Adapting equation (11), we find for T much larger than the half-life of ^{36}Cl

$$^{36}Ar/^{36}Cl = [\lambda P_{^{36}Ar} T]/[P_{^{36}Cl}(1 - e^{-\lambda T})] \quad (17)$$

where the term $P_{^{36}Ar}$ includes the indirect contribution from the decay of ^{36}Cl, about 83.5% of the total. Equation (17) incorporates the approximation that all ^{36}Cl produced has already decayed, mostly to ^{36}Ar. This approximation introduces a negligible error for meteorites with CRE ages >10 m.y., but a slightly more complex equation applies to meteorites with short CRE ages (*Nyquist et al.,* 1973).

Direct cross-section measurements at various energies for the nuclear reactions such as Fe(p,x)^{36}Ar and Fe(p,x)^{36}Cl give fairly good estimates for the production rate ratio in iron meteorites or the metal phases of stony ones (*Lavielle et al.,* 1999).

On conversion to measurement units, *Albrecht et al.* (2000) obtained the equation

$$T = (430 \pm 16) \times (1 - e^{-\lambda_{36} T}) \times \frac{^{36}Ar}{^{36}Cl} \quad (18)$$

where ^{36}Ar is inserted in units of 10^{-8} cm^3 STP/g metal and ^{36}Cl in dpm/kg metal. *Lavielle et al.* (1999) recommend a very similar constant of 427.

3.3.4. Potassium-40/potassium-41 cosmic-ray exposure ages. Although the method based on ^{40}K/^{41}K systematics is the most complex, it is important for the study of the long-term constancy of the cosmic radiation. *Voshage* (1967) developed the method (equation (19)) during the period from about 1960 to 1985 and applied it mainly to irons and the metal phases of stony irons with CRE ages greater than about 100 m.y.

$$^{41}K/^{40}K - c^{39}K/^{40}K = (P_{41}/P_{40} - cP_{39}/P_{40})\lambda T/(1 - e^{-\lambda T}) \quad (19)$$

where the constant c is the primordial $^{41}K/^{39}K$ ratio in the meteorite and λ the ^{40}K decay constant.

The first term on the righthand side of equation (19) represents a shielding-dependent production-rate ratio, as discussed by *Voshage and Hintenberger* (1963). The evaluation is not straightforward since we do not know the relevant nuclear cross sections. These authors estimated production-rate ratios under various shielding conditions from theoretical model calculations and using measured $^{4}He/^{21}Ne$ ratios as the shielding parameter, permitting a relation between the K-production-rate ratios and the $^{4}He/^{21}Ne$ ratios. Using a least-squares fitting procedure and considering only data for meteorites with one-stage exposure histories, *Lavielle et al.* (1999) revisited the evaluation of $^{41}K/K$ ages.

The CRE ages obtained from equations (12), (17), and (19) are not sensitive to matrix effects, since these equations involve the ratio of two nuclides produced by similar nuclear reactions. In this context, "similar" means that the two nuclides are produced from the same set of target elements and that the cross sections for the relevant nuclear reactions depend on energy in similar ways. Although in reality variations in the behavior of the cross sections are to be expected, their effects on the exposure ages appear to be smaller than present measurement uncertainties.

3.4. Complex Exposure Histories

The one-stage irradiation model for meteorites has proved quite robust. As we shall demonstrate in section 4, good evidence for it comes from the clustering of CRE ages, as exemplified by the 6–8-m.y. peak in the H-chondrite CRE age distribution. In numerous instances, however, meteoritic inventories of cosmogenic nuclides also include sizeable contributions from earlier periods of irradiation. Such meteorites are said to have had complex exposure histories, with successive stages presumably initiated by collisions that changed the geometric conditions of irradiation and hence production rates. To comply with space limitations, we give only an overview of this subject, moving backward in time.

1. Meteoroids may undergo collisions in space. A collision will usually decrease the size of the irradiated object, and as a result, average GCR production rates will increase in most instances. If the longer-lived and stable nuclides are retained, they record both the earlier and later stages of irradiation. The relative contributions from the two stages depend, of course, on the durations and the shielding conditions. In contrast, the shorter-lived radionuclides produced in the earlier stages have time to decay before Earth arrival. For meteorites that have had a two-stage irradiation, the nominal one-stage CRE ages calculated for longer-lived nuclides will be larger than the CRE age calculated from the shorter lived nuclides. Examples include the meteorites Pitts (*Begemann et al.,* 1970), Bur Gheluai (*Vogt et al.,* 1993a), Torino (*Wieler et al.,* 1996), Shaw (*Herzog et al.,* 1997), Peekskill (*Graf et al.,* 1997), and Kobe (*Caffee et al.,* 2000; *Goswami et al.,* 2001).

Erosion in space can be regarded as special type of complex history characterized by a multitude of small, virtually continuous, size-reducing collisions. Erosion is well established in lunar rocks (*Hörz et al.,* 1991) and is typically estimated to be ~1 mm/m.y. Erosion rates of meteoroids were inferred to be somewhat lower, 0.65 mm/m.y. for stones and 0.022 mm/m.y. for irons (*Schaeffer et al.,* 1981; *Welten et al.,* 2001a).

2. Proto-meteoroids may undergo irradiation as parts of large fragments in parent-body regoliths. Such irradiation is detectable as neutron-capture effects in the meteoritic matter (see also section 2). In particular, the aubrites show evidence for preexposure on their parent body. For the Norton County aubrite, *Eugster et al.* (1970) found anomalies in the Gd-isotopic composition due to neutron capture of ^{157}Gd. Subsequently, these effects in the form of Sm- and Gd-isotopic shifts were observed by *Hidaka et al.* (1999) for five aubrites. These authors concluded that the meteoritic matter was located near the surface of its parent body for several hundred million years. *Lorenzetti et al.* (2003) confirmed the high neutron fluxes experienced by many aubrites: Excesses of neutron-produced ^{80}Kr were measured in Shallowater, Khor Temiki, Cumberland Falls, and Mayo Belwa, the latter two also showing the above-mentioned Sm- and Gd-isotopic shifts. The neutron-exposure time must have been considerably longer than the time indicated by the CRE age, requiring a regolith history for the aubritic matter before compaction into the present meteorite.

Herzog (2003) suggests that an appreciable number of micrometeorites likely belong in this group and retain records of surface exposure on parent bodies in the relatively recent past. *Pepin et al.* (2001) discuss other possible CRE histories for micrometeorites.

For the other end of the size scale, *Welten et al.* (2004) propose that several large meteorites with complex histories were irradiated essentially as boulders on parent-body surfaces. Meteorites in this group include Tsarev (*Herzog et al.,* 1997), Jilin (*Heusser et al.,* 1996), Gold Basin (*Welten et al.,* 2003), and QUE 90201 (*Welten et al.,* 2004). The criteria for distinguishing between irradiation in a boulder on a parent body and a boulder orbiting in space, i.e., between our cases (1) and (2), are not well defined.

3. Small, independent meteorite grains (<1 mm) may undergo irradiation on parent-body surfaces or even in other meteoroids prior to compaction into the matter that becomes the meteorite studied. Many meteorites contain gases implanted by SW and SCRs, which as noted earlier, travel only a few millimeters in matter. Thus the presence of solar gases implies exposure to GCR as well. Good examples are some aubrites that contain solar gases and neutron-produced nuclides, indicating that they have been located near the surface of their parent body (*Hidaka et al.,* 1999; *Lorenzetti et al.,* 2003). *Hohenberg et al.* (1990) showed that small, solar-gas-rich grains in carbonaceous chondrites contain more GCR-produced ^{21}Ne than do samples of the corresponding bulk meteorites. The timing and intensity of the early irradiation is controversial (*Rao et al.,* 1997; *Wieler et al.,* 2000),

although it seems likely that compaction occurred very early in the history of the solar system.

As recognized early on, meteoritic breccias may also contain somewhat larger fragments from various sources, not all of which contain solar noble gases, and each with its own irradiation history. A few examples of meteorites in this category include Weston (*Schultz et al.,* 1972), St. Mesmin (*Schultz and Signer,* 1977), Fayetteville (*Wieler et al.,* 1989; *Padia and Rao,* 1989; *Nishiizumi et al.,* 1993b), and possibly Kaidun (*Kalinina et al.,* 2004).

4. Components of meteorites may have undergone irradiation not in regoliths, but as free-floating bodies in the early solar nebula. *Polnau et al.* (2001) showed that chondrules in several meteorites contain more GCR-produced nuclides than the average bulk meteorites from which they come. They attribute the excesses to a 4π irradiation shortly after chondrule formation and before incorporation in a parent body. Certain theoretical models explain the abundances of now-extinct radionuclides in meteoritic matter (inclusions rich in Ca and Al and chondrules) by postulating an early irradiation close to an active ancient Sun (*Gounelle et al.,* 2001, 2004; *Leya et al.,* 2003; *Chaussidon and Gounelle,* 2006).

5. Extrasolar grains preserved in meteorites must have been irradiated in interstellar space. *Ott and Begemann* (2000) discuss this challenging frontier of CRE ages.

3.5. Time Variations

Evidence of variations of the particle environment, i.e., in the flux of GCRs and of the energetic particles emitted by the Sun, is recorded in meteorites for two endpoints in the evolutionary history of the solar system: the earliest stages of the solar nebula and the last 1 G.y. The variation of the particle environment in the early solar nebula is a separate chapter in this book (*Chaussidon and Gounelle,* 2006). We consider here the more recent changes. Shock acceleration from supernovae explosions is now considered to be a major source of the GCRs (*Reeves,* 1978; *Axford,* 1981; *Ramaty et al.,* 1996; *Ustinova,* 2002). The observed differential stellar motions in active star-forming regions can be used to reconstruct the past locations of supernovae and therefore the particle environment of the solar system (*De Zeeuw et al.,* 1999; *Branham,* 2002).

It has long been recognized that iron meteorites are excellent fossil detectors of cosmic radiation. Their CRE ages are calculated from a substantial database of GCR-produced nuclides that includes the data used for the $^{40}K/^{41}K$ method discussed earlier (*Voshage,* 1967; *Voshage and Feldmann,* 1979; *Voshage et al.,* 1983). Interestingly, several studies indicate systematic differences between ages obtained by stable nuclides and radioactive nuclides of with different half-lives, such as $^{36}Cl/^{36}Ar$, $^{39}Ar/^{38}Ar$, $^{10}Be/^{21}Ne$, and $^{129}I/^{129}Xe$ when compared to the $^{40}K/^{41}K$ CRE ages. These discrepancies have been interpreted as evidence for a time-variation in the GCR flux (*Marti et al.,* 2004). However, alternative interpretations, such as erosion in space and complex exposure histories of iron meteorites (*Voshage,* 1982; *Lavielle et al.,* 1999), need to be considered.

Lavielle et al. (1999) used an approach in the evaluation of the constancy of GCRs that eliminates irons with complex exposure histories. They assume a constant GCR flux over a limited time interval of 150–700 m.y. ago, but then find that meteorites with longer exposure ages are in conflict with this assumption.

To summarize, CRE ages of iron and stony iron meteorites based on the ^{40}K half-life disagree in a systematic way with radionuclides of <5-m.y. half-lives, such as ^{81}Kr, ^{36}Cl, ^{10}Be, and ^{53}Mn (e.g., *Eugster,* 2003). The average production rates of ^{36}Cl or ^{36}Ar over the time interval of 150–700 m.y. inferred for CRE ages based on K isotopes are lower by 28% when compared to production rates commonly used for the recent GCR flux. A recent GCR flux increase offers a most straightforward explanation. A new alternative calibration of interest for recent variations in the GCR flux is proposed based on the 16-m.y. radionuclide ^{129}I, which decays to ^{129}Xe (*Marti,* 1986; *Marti et al.,* 2004). Iodine-129 is efficiently produced by neutron reactions on Te that is mainly located in troilite. *Schnabel et al.* (2004) modeled the production of ^{129}I in stony meteorites based on experimental production rates of ^{129}I from thick-target experiments. Iodine-129 integrates the GCR flux over several half-lives and is thus well suited to study the flux records during the last 100 m.y.

4. COSMIC-RAY EXPOSURE AGES

Most CRE ages are calculated from noble gas data. The latest compilation (*Schultz and Franke,* 2004) gives He-, Ne-, and Ar-isotopic abundances for more than 1600 meteorites. For the calculation of CRE ages <4 m.y., radionuclide data are also used in particular for CM and CI chondrites (*Nishiizumi and Caffee,* 2002) for which large trapped-noble-gas contributions make the quantification of the GCR-produced component difficult.

Dynamical aspects and orbital evolution considerations are required for the understanding of the systematics in CRE age distributions. A decade ago it was thought that transit times to Earth are determined by proximity and injection of the meteoroid into "chaotic resonances in the inner main belt" (e.g., *Bottke et al.,* 2000). Such dynamics may account for longer exposure ages of stony irons and irons and possibly the low ^{3}He concentrations of not only irons, but also H5 chondritic metals (*Graf et al.,* 2001). These authors showed that metal in some H5 chondrites had been heated to temperatures where ^{3}H was diffusing out of the metal, requiring orbits with close approaches to the Sun. The chaotic injection model failed to explain some observed properties of asteroids (*Bottke,* 2002) and especially the long CRE ages for implied orbits with solar heating effects. Calculations by *Gladman* (1997) showed that once a meteoroid's orbit is in a resonance with that of Jupiter, its orbit quickly evolves to an Earth-crossing one. Consideration of the Yarkovsky effect seems to resolve several problems

(*Farinella et al.,* 1998; *Vokrouhlicky et al.,* 2000; *Spitale and Greenberg,* 2002). The Yarkovsky effect, the asymmetric heating of meteoroids by solar radiation, leads to small forces of acceleration that change the principal elements of the meteoroid orbit. The changes occur slowly enough that a meteoroid may spend tens of millions of years or more in the main belt before it reaches a resonance that brings it to the inner solar system, specifically to Earth. Smaller orbital changes by the Yarkovsky effect are expected for irons because of their optical properties, which would allow for longer random-walk passages through the main belt. Although most physical parameters that control CRE age distributions are understood, we should not forget that the ejection of meteoroids begins with random collisional events on parent objects, which account for the general clumpiness of the CRE age distributions.

Several lines of evidence (chemical, mineralogical, textural, and isotopic) indicate that the meteorites in the world's collections came from about 15 unmelted (undifferentiated, chondritic) asteroids and possibly 70 melted (differentiated) asteroids (*Keil et al.,* 1994; *Burbine et al.,* 2003). We discuss the CRE age histograms of several different meteorite classes. These data are used to obtain collisional information, constraints on their origin and parent-body history, break-up events, and ejection of meteorites, as well as on the dynamical systematics of their immediate precursor bodies.

4.1. Chondritic Meteorites

4.1.1. H, L, LL, E, and R chondrites. The CRE ages of the three major "ordinary" (H, L, LL) types of chondrites were reviewed by *Marti and Graf* (1992) and the CRE age histograms of these meteorites are presented in Fig. 4. These authors showed that none of the histograms is consistent with a continuous delivery of asteroidal material to Earth, as the observed CRE data clearly disagree with expected exponential distributions for a variety of orbital lifetimes. They conclude that CRE age histograms are dominated by stochastic events and that the continuous supply of asteroidal material can account for only a minor background. It is difficult therefore to infer collisional or dynamical half-lives for chondrite populations from measured histograms. The H chondrites recorded two major events, ~7 m.y. and ~33 m.y. ago; among the L chondrites, events at ~28 m.y. and ~40 m.y. ago were identified, and the LL chondrites suffered a collision ~15 m.y. ago.

Graf and Marti (1995) conclude that very few H chondrites have exposure ages of less than 1 m.y. The CRE age distribution of H chondrites is consistent with the production of H chondrites by a relatively small number of events involving only a few parent bodies. Orbital information can be obtained from the p.m./total fall ratio among observed falls: H3, 4, and 6 chondrites show the typical afternoon excess of falls, but the H5 subgroup reveals a clear exception with a ratio of p.m./total falls <0.5. This ratio of fall times suggests the possibility of two collisional events, and an evolved orbit for one H5 parent object involved in the 7-m.y. collisional events. These authors further point out that for each petrologic type, there is a similar fraction of gas-rich stones. The implanted solar-type noble gases indicate that the gas-rich material had a regolith history. *Graf and Marti* (1995) conclude that the immediate parent of H chondrites was not an ancient layered object, since in this case the higher petrographic types should be devoid of solar-type noble gases, contrary to observation.

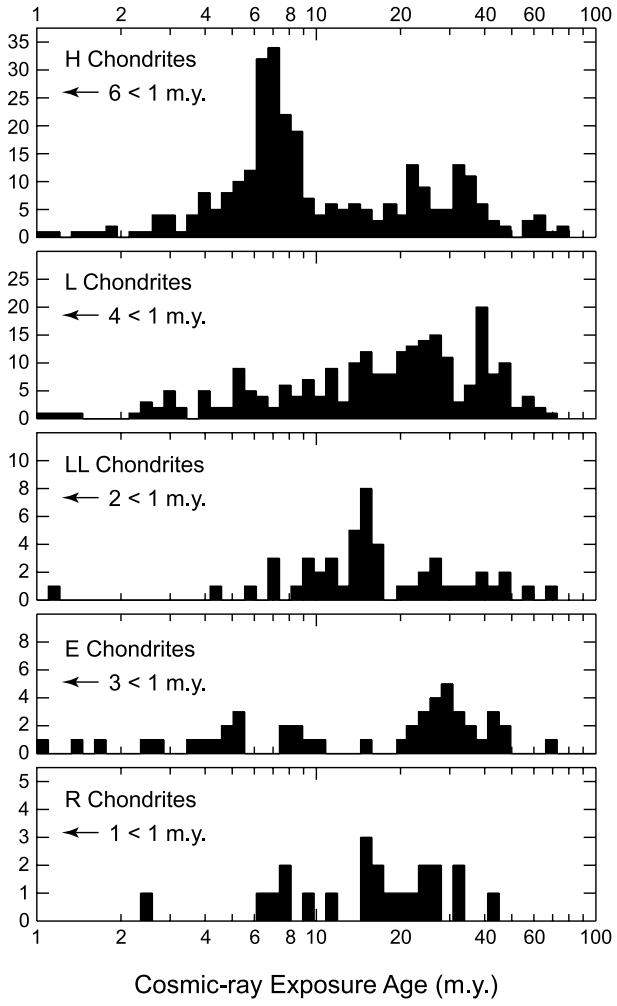

Fig. 4. Cosmic-ray exposure age distributions for H, L, LL, enstatite, and Rumuruti-type chondrites. Ordinary chondrite data are from *Marti and Graf* (1992), *Graf and Marti* (1994, 1995), and updates; the E-chondrite histogram is from *Patzer and Schultz* (2001) and that for the R chondrites from *Schultz et al.* (2005). Off-scale numbers of meteorites are indicated by arrows.

Marti and Graf (1992) reviewed L-chondrite exposure ages and, as in the case of H chondrites, the CRE age histograms (Fig. 4) of L5 and L6 chondrites do not fit a continuum; they also differ for the petrologic types. A strong CRE age peak occurs at about 40 m.y., a less well-defined peak is at 5 m.y., and a broad peak runs from 20 to 30 m.y. with a maximum in the vicinity of 28 m.y. All L3 or L4 CRE ages are <50 m.y. Many L chondrites have lost radiogenic

^{40}Ar and ^{4}He. Numerous authors have searched for relations between these gas losses and CRE ages. The CRE age peaks at 5 m.y. and 28 m.y. noted above stand out much more clearly for L chondrites that exhibit significant losses of ^{40}Ar than for other L chondrites. This difference in turn suggests that these events sampled strongly heated portion(s) of the L-chondrite parent body or bodies.

Okazaki et al. (2000) studied the light noble gases in 11 enstatite (E) chondrites and found CRE ages (based on ^{21}Ne) divided in two groups: <15 m.y. and >40 m.y. *Patzer and Schultz* (2001) reported ^{21}Ne CRE ages of about 60 E chondrites. This distribution (Fig. 4) is somewhat similar to that of the L chondrites, but clearly differs from the CRE age histogram of enstatite achondrites, the aubrites (Fig. 6). *Patzer and Schultz* (2001) identified clusters at about 3.5, 8, and 25 m.y., but caution that confirmation is needed. The CRE ages show no systematic correlation with either petrologic type or iron content (high-iron enstatites, EH chondrites; low-iron enstatites, EL chondrites). Thus, the CRE age distribution of the E chondrites yields no information on the structure of the E-chondrite parent asteroid.

The CRE ages of 23 individual R-chondrite falls (Fig. 4) range from 0.2 to 42 m.y. Six of them cluster at 16.6 ± 1.1 m.y. and may suggest a breakup on their parent body (*Schultz et al.,* 2005). Eleven of these meteorites contain solar gases and are thus regolith breccias. This percentage of almost 50% is higher than that of ordinary chondrites, howardites, and aubrites and may imply that the parent body of the R chondrites has a relatively thick regolith.

4.1.2. Carbonaceous chondrites. Most CI and CM chondrites have very short CRE ages of <2 m.y. (Fig. 5). Only the lunar meteorites have similarly short ages. *Scherer and Schultz* (2000) discuss three possible reasons why meteorites have short exposure ages: (1) the parent body was close to a resonance, (2) the parent body was in an Earth crossing orbit when a collision ejected the meteoroid, (3) their fragile character diminishes the rate of survival in space. The CRE ages of CI and CM chondrites are largely based on data from cosmogenic radionuclides. Based on ^{26}Al and ^{10}Be measurements, *Caffee and Nishiizumi* (1997) report a CRE age peak at 0.2 m.y. for C2 (mostly CM) meteorites. No peak is observed in the distribution of ^{21}Ne ages, but this may reflect the uncertainties in spallation noble gas components in CI and CM chondrites, which are affected by components from earlier irradiations (see section 5).

The average CRE (^{21}Ne) ages for CV, CK, and CO chondrites (not corrected for pairing) are 13 ± 10, 23 ± 14, and 22 ± 18 m.y., respectively. These ages are about one order of magnitude larger than those of the CI and CM chondrites. Cosmic-ray exposure measurements of other clans of carbonaceous chondrites (CR, CH, and CB) are rare, and data are not shown in Fig. 5. Cosmic-ray exposure ages for the CR and CH chondrites range from 1 to 25 m.y. and 1 to 12 m.y., respectively, while those of the CB chondrites Bencubbin (*Begemann et al.,* 1976) and Gujba (*Rubin et al.,* 2003) are about 30 m.y.

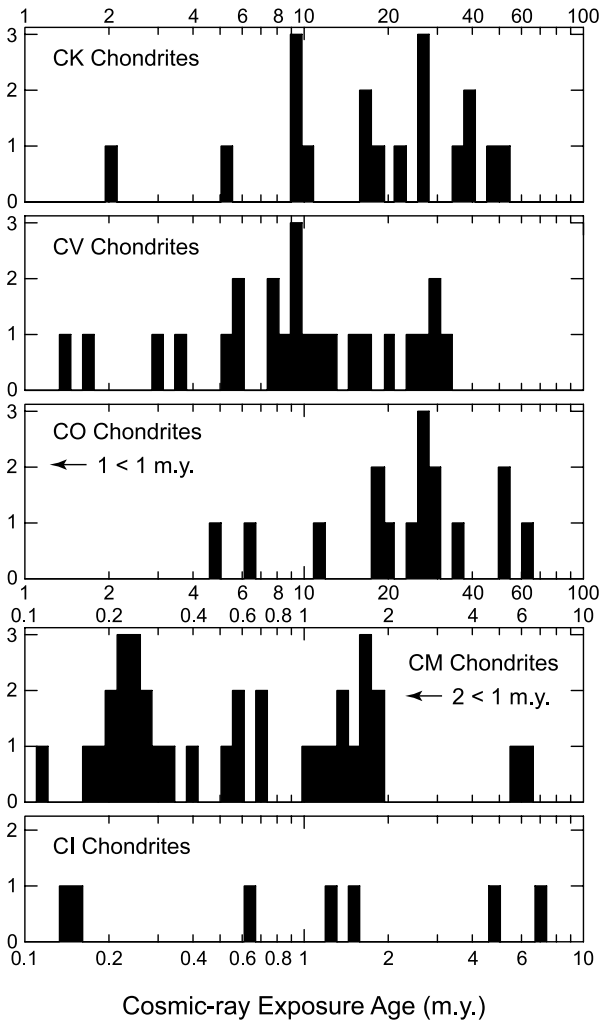

Fig. 5. Cosmic-ray exposure age distributions for carbonaceous chondrites. Data for CK, CV, and CO chondrites are from *Scherer and Schultz* (2000); a few updates are included. Data for CM chondrites from *Nishiizumi et al.* (1993a), *Caffee and Nishiizumi* (1997), *Eugster et al.* (1998), and *Nishiizumi and Caffee* (2002). Data for CI chondrites from *Nishiizumi et al.* (1993a) and K. Nishiizumi (personal communication, 2001).

4.2. Achondritic Meteorites

4.2.1. Howardites, eucrites, and diogenites (HED meteorites). The CRE age histogram of the HED meteorites shown in Fig. 6 reveals the following clusters: All three types of HED meteorites are represented in the 22 ± 3 m.y. age peak and in a cluster at 36 ± 3 m.y., while eucrites cluster also at 12 ± 3 m.y.; two eucrites and one diogenite have CRE ages of 7 ± 1 m.y. Of all 86 dated HEDs, at least 70% fall in these four clusters and more, if only ^{81}Kr-Kr ages are considered. For discussions of the statistical significance of the observed CRE age clusters see the original literature (*Eugster and Michel,* 1995; *Shukolyukov and Begemann,*

1996; *Welten et al.,* 1997). The rather similar histograms for H, E, and D clans suggest collisional breakup processes and ejections from the same parent object(s).

Asteroid Vesta was suggested as the common parent of the HEDs (*Consolmagno and Drake,* 1977), but transfers from Vesta to Earth appear to be dynamically difficult. A possible solution to the dynamical problem was proposed by *Binzel and Xu* (1993): a two-step evolution of orbital elements. These authors discovered several small asteroids with diameters of 5–10 km of basaltic achondritic composition with semimajor axes ranging between those of Vesta and the distance of the 3:1 resonance with Jupiter. They conclude that injection of large (>1 km) fragments into this resonance for subsequent delivery of meteoritic material to the inner solar system might explain the transfer dynamics. In this case the common ejection times of HEDs would imply that multikilometer-sized objects contain eucritic, diogenitic, and howarditic materials. *Bottke et al.* (2000) pointed out that the typical CRE ages of the HEDs (10–40 m.y.) are consistent with estimates obtained based on the Yarkovsky effect (see below) and Vesta as the parent object. In case of a model where HEDs were delivered directly from Vesta to Earth, the collisional events at 22 m.y., 12 m.y., and 36 m.y. must have been large, since they must liberate simultaneously Vesta's surface (eucrites, howardites) and interior (diogenites) layers. Smaller and frequent collisional events can be expected to eject only eucrites and howardites, a scenario consistent with the CRE age clusters.

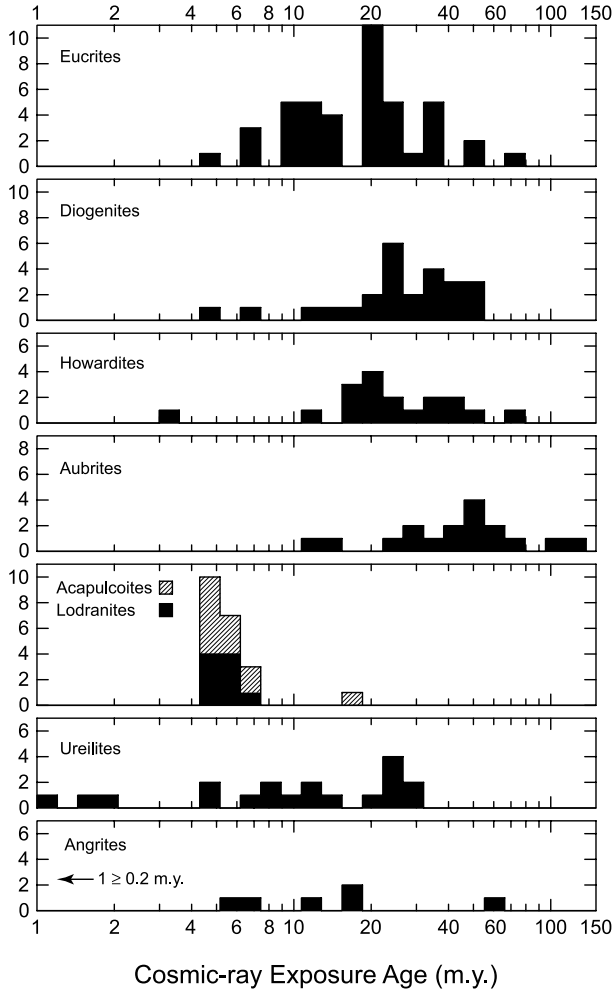

Fig. 6. Cosmic-ray exposure age distributions for achondrites. Data for eucrites, diogenites, and howardites were taken from *Eugster and Michel* (1995), *Miura* (1995), *Shukolyukov and Begemann* (1996), *Welten et al.* (1997), *Miura et al.* (1998), *Caffee and Nishiizumi* (2001), and *Welten et al.* (2001a); for aubrites from *Lorenzetti et al.* (2003); for acapulcoites and lodranties from *Weigel et al.* (1999), *Terribilini et al.* (2000a), and *Patzer et al.* (2003); for ureilites from *Goodrich* (1992) and *Scherer et al.* (1998); for angrites from *Eugster et al.* (2002b).

4.2.2. Aubrites (enstatite achondrites). The CRE ages of aubrites range from 12 to 116 m.y. (Fig. 6) and their distribution is nonuniform. Although a cluster appears around 50 m.y., an implied collisional event is highly doubtful, as seven of the eight aubrites with ages between 40 and 60 m.y. are breccias (*Lorenzetti et al.,* 2003). Six of these show characteristics of precompaction regolith exposure, chondritic inclusions, shock blackening, implanted solar noble gases in the surface layers of regolith grains, or isotopic variations produced by neutron capture (e.g., Sm, Gd, Br; see section 2). The two aubrites with the longest CRE ages of all stone meteorites, Norton County and Mayo Belwa, were not exposed to the solar wind. The relatively long CRE ages of aubrites (given their low physical strength) suggest that orbital elements of their parent body are distinct from those of other classes of stone meteorites. Specifically, the origin of the enstatite chondrites, with nearly half of their CRE ages <10 m.y., must differ from that of the enstatite achondrites, as first pointed out by *Eberhardt et al.* (1965).

4.2.3. Acapulcoites and lodranites. For no other meteorite group do the CRE ages cluster as tightly as for the acapulcoites and lodranites (Fig. 6). This clustering suggests ejection from a parent body in a breakup event about 6 ± 1.5 m.y. ago (*Terribilini et al.,* 2000a). Some fine structure in CRE age peak exists (*Eugster and Lorenzetti,* 2005), and there is an additional CRE age of 15 m.y. (*Patzer et al.,* 2003). Several other lines of evidence indicate that the acapulcoites and lodranites originated from a common parent body (*McCoy et al.,* 1997). *Eugster and Lorenzetti* (2005) proposed a model in which acapulcoites originate from the outer layer where the temperature was never high enough for silicate partial melting, accounting for old ^{39}Ar-^{40}Ar ages of 4503–4556 m.y., while lodranites would represent the inner shell of their parent asteroid, with ^{39}Ar-^{40}Ar ages at the later end of this range.

4.2.4. Ureilites. Ureilites share several properties characteristic of primitive meteorites, e.g., concentrations of heavy noble gases and O-isotopic signatures representing primitive solar system materials (*Scherer et al.,* 1998). The CRE age distribution of ureilites ranges from ~0.1 to about 34 m.y. (Fig. 6) and show no age clusters that would indi-

cate breakup events; however, statistics are still poor. The large spread in CRE ages and the evidence for regolith evolution (some breccias contain solar gases) suggest a relatively large parent asteroid.

4.2.5. Angrites and brachinites. Cosmic-ray exposure ages are available for seven of the nine known angrites (Fig. 6). Statistics for CRE ages are poor, but suggest ejection events 6, 12, 17, and 56 m.y. ago (*Eugster et al.,* 2002b). Approximate CRE ages are available for three of seven known brachinites (not shown in Fig. 6): Brachina, 3 m.y. (*Ott et al.,* 1985); ALH 84025, 10 m.y. (*Ott et al.,* 1987); and Eagles Nest, 25 m.y. (*Swindle et al.,* 1998).

4.3. Stony-Iron Meteorites

Cosmic-ray exposure ages based on noble gases and cosmogenic radionuclides are available for mesosiderites (*Begemann et al.,* 1976; *Terribilini et al.,* 2000b; *Albrecht et al.,* 2000; *Nishiizumi et al.,* 2000; *Welten et al.,* 2001b). Figure 7 shows the distribution of the CRE ages for the mesosiderites and pallasites. The average, ~90 m.y., is intermediate between CRE ages for stones (younger) and irons (older). The age distribution has no obvious clusters, but *Welten et al.* (2001b) note that 3 of 19 mesosiderites have CRE ages close to 70 m.y.

4.4. Iron Meteorites

A long space exposure is evident for most, but not all, iron meteorites that record CR histories during the last ~1 G.y. Many also show multistep exposure histories. Cosmic-ray exposure ages for the four main groups I–IV are shown in Fig. 8.

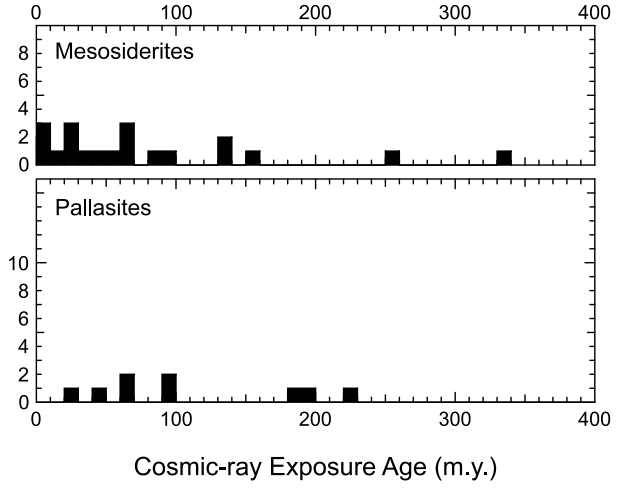

Fig. 7. Cosmic-ray exposure age distributions for stony-iron meteorites. Data for the mesosiderites are from *Begemann et al.* (1976), *Albrecht et al.* (2000), *Terribilini et al.* (2000b), and *Welten et al.* (2001b); for pallasites from *Megrue* (1968), *Voshage and Feldmann* (1979), *Shukolyukov and Petaev* (1992), and *Honda et al.* (1996).

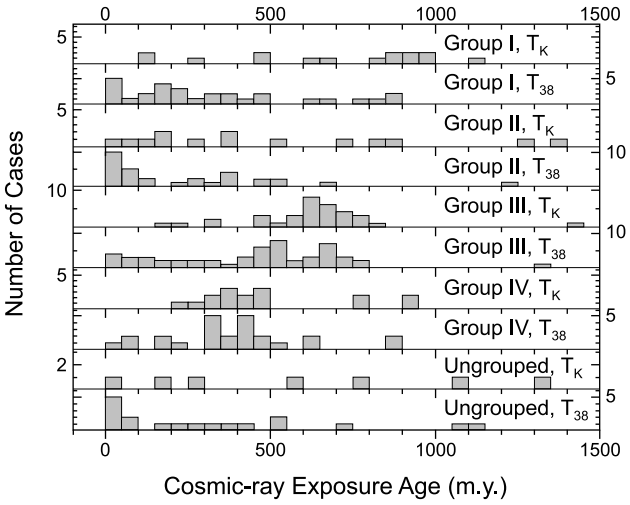

Fig. 8. Cosmic-ray exposure ages of iron meteorites. The ^{40}K/K ages (T_K) are from *Voshage* (1967), *Voshage and Feldmann* (1979), and *Voshage et al.* (1983). The ^{38}Ar–^{4}He/^{21}Ne ages are from *Lavielle et al.* (1985).

As noted above, CRE ages based on Ar data and those based on K disagree in a systematic way (*Schaeffer et al.,* 1981; *Lavielle et al.,* 1999). Potassium-40/potassium-41-based CRE ages are less accurate for ages <200 m.y. because of limitations inherent to the method and to the experimental technique. There are few irons with CRE ages >1 G.y. For group III irons, both the ^{40}K/K- and the ^{38}Ar-based CRE ages cluster at about 650 m.y.; the ^{38}Ar-based CRE ages suggest a second peak at about 450 m.y. (*Lavielle et al.,* 1985). *Lavielle et al.* (1999) documented a peak in CRE ages of IVA irons based on ^{40}K/^{41}K ages and more recently *Lavielle et al.* (2001) resolved this peak into two clusters at 255 ± 15 m.y. and 217 ± 13 m.y., respectively, using data obtained by the ^{36}Ar/^{36}Cl method.

4.5. Martian Meteorites

At present about 50 meteorites representing about 30 individual falls of meteorites whose parent body is Mars have been recovered. In a comprehensive review on ages and geological histories of martian meteorites, *Nyquist et al.* (2001) discussed the characteristics of crystallization age and isotopic and elemental composition, as well as the arguments for their martian origin.

The martian meteorites can be divided into seven petrographic types, characterized, e.g., by their ratio of pyroxene to olivine (*Meyer,* 2003): basaltic shergottites (average px/ol = 400), olivine-phyric shergottites (3.3), lherzolites (0.77), clinopyroxenites (nakhlites, 5.5), a dunite (only member Chassigny, 0.05), an orthopyroxenite (only member ALH 84001, ≫100), and EET 79001, consisting of two main lithologies of olivine-phyric and of basaltic composition, respectively. Figure 9 shows that these meteorites were ejected in a number of discrete events. The earliest event

is represented by Dhofar 019, an olivine-phyric shergottite, 19.8 ± 2.3 m.y. ago. The only orthopyroxenite, ALH 84001, has an ejection age of 15.0 ± 0.8 m.y. It is the only meteorite from the ancient martian crust (for references see *Nyquist et al.,* 2001). All five clinopyroxenites (nakhlites), consisting primarily of magnesian augite with lesser amounts of Fe-rich olivine, have a common ejection age of 10.6 ± 1.0 m.y. The same impact event may also be responsible for the only dunite (Chassigny) since its T_{ej} is 11.1 ± 1.6 m.y. The six basaltic shergottites yield ejection ages in the range of 2.4–3.0 m.y. They consist predominantly of the clinopyroxenes pigeonite and augite and differ from the four lherzolites that consist mainly of olivine, orthopyroxene, and chromite. Lherzolites were ejected 3.8–4.7 m.y. ago. *Nyquist et al.* (2001) also discuss the possibility that the lherzolites were preexposed on the martian surface and that they were ejected at the same time as the group of basaltic shergottites. However, there is no evidence from radionuclide activities (*Schnabel et al.,* 2001) that supports such a scenario. Five olivine-phyric shergottites were ejected 1.2 ± 0.1 m.y. ago. Finally, the ejection age of EET 79001 is 0.73 ± 0.15 m.y. (*Nyquist et al.,* 2001). We conclude that eight events may account for the ejection of the martian meteorites, if Chassigny was not ejected together with the nakhlites.

Model calculations for the transfer times of rocks ejected from Mars are consistent with the distribution of observed CRE ages for material ejected slightly above escape velocity of 5 km/s. *Gladman et al.* (1996) found that 95% of all ejected rocks reach Earth within 20 m.y. and only about 20% are expected to have CRE ages <1 m.y. In contrast to lunar meteorites (see below), no clear evidence for a complex exposure history has been observed for martian meteorites. If the impacts on Mars occur at few-million-year intervals, as indicated by the CRE ages, the size of the impactors are likely to be on the order of kilometers and the resulting craters tens of kilometers in diameter (*Gladman,* 1997). Thus, most ejected rocks are expected to originate from more than a few meters depth and did not experience a preexposure to cosmic rays on Mars. The size of the ejected rocks from such impacts is estimated to be in a range of 20–200 cm (*Artemieva and Ivanov,* 2002; *Eugster et al.,* 2002a). Consequently, the number of martian meteoroids from a cratering event must be enormous, and source crater pairing of specimens collected on Earth is not surprising.

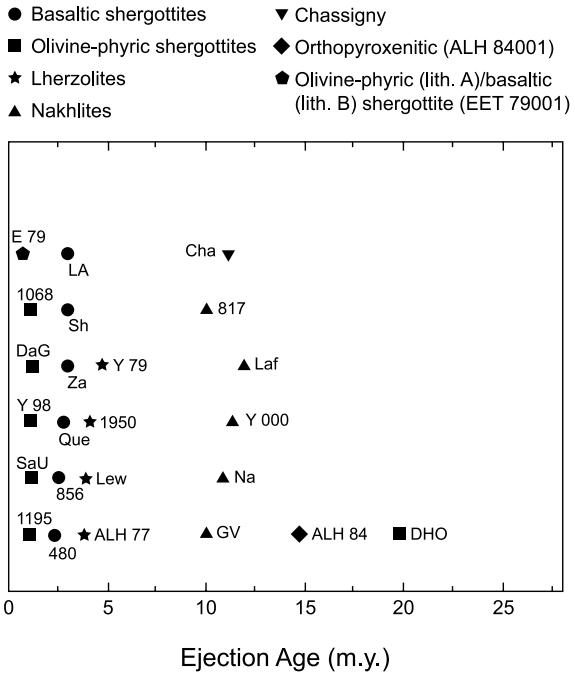

Fig. 9. Ejection ages of martian meteorites. For references of data source and meteorite names see *Meyer* (2003).

4.6. Lunar Meteorites

During the past two decades numerous (more than 40) lunar meteorites were found in several different locations, including Antarctica, North Africa, Oman, and Australia. These stones were blasted off the Moon by impacts and are identical in all relevant characteristics with the specimens returned by the Apollo missions.

Although lunar meteorites fell at different locations at different times, some of them may originate from the same lunar cratering event, i.e., they may be source-crater paired. The relevant parameter for judging source-crater pairing, the ejection age, is the sum of the Moon-Earth transfer time and the terrestrial age. Source-crater pairing is further constrained by the chemical characteristics of the meteorites.

Figure 10 shows measured Ca/Ti elemental ratios vs. ejection ages (*Lorenzetti et al.,* 2005). This ratio is chosen because in highland rocks the Ca concentration is higher and that of Ti lower than those in mare material. Several groupings are identified for meteorites with similar Ca/Ti ratios and ejection ages: the five highland breccias, DaG 400, QUE 93069/94269 (fall paired), DaG 262, ALHA 81005, and Y 791197 all have ejection ages of 0.06 m.y., and source-crater pairing cannot be excluded; MAC 88104/88105 (fall paired) and NWA 482 have T_{ej} = 0.25–0.30 m.y.; Y 82192/82193/86032 (fall paired) have T_{ej} = 8 ± 3 m.y. For the mare basalts and the highland/mare rocks we observe five different ejection ages: Y 793274 and Y 981031 are paired and have T_{ej} < 0.04 m.y.; EET 87521/96008 (fall paired) T_{ej} = 0.05 to 0.11 m.y.; QUE 94281 T_{ej} = 0.35 ± 0.10 m.y.; both Asuka 881757 and Y 793169 have T_{ej} = 1.0 ± 0.2 m.y., and Calcalong Creek 3 ± 1 m.y. From these data we conclude that at least three impact events in highland areas and five events in mare regions ejected the lunar meteorites collected until now.

The escape speed for rocks ejected from the Moon is 2.4 km/s. About 97% of all rocks ejected with ≤3.2 km/s reach the Earth within <1 m.y. (*Arnold,* 1965; *Gladman et al.,* 1995) and only a small fraction of all rocks is launched at speeds >3.2 km/s (*Gladman et al.,* 1996). *Warren* (1994) concluded that most lunar meteorites are ejected by impact

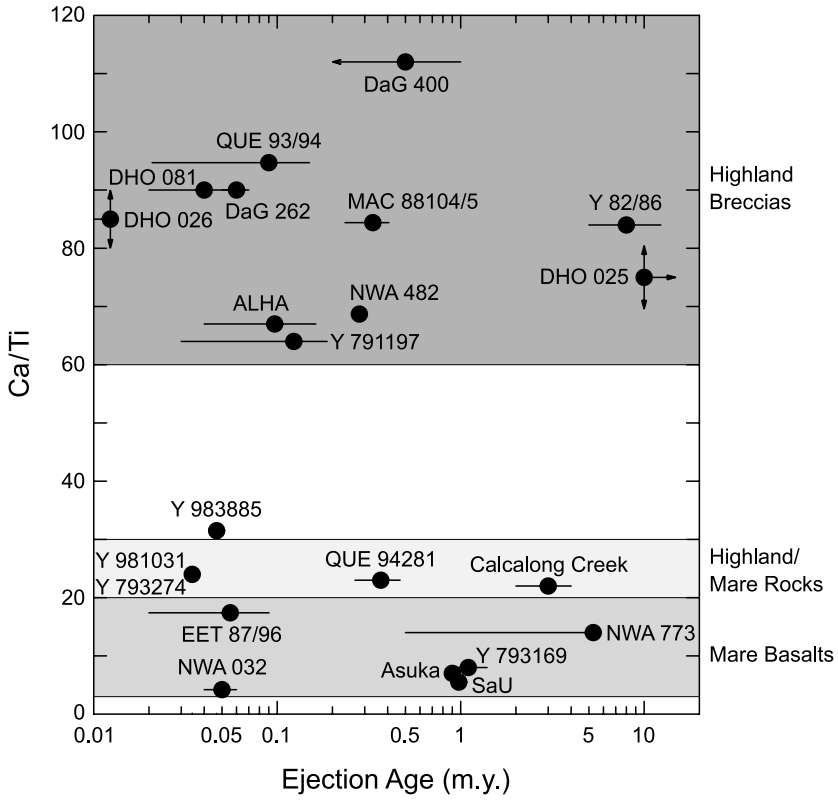

Fig. 10. Calcium/titanium ratios of lunar meteorites vs. times of ejection from the lunar surface. This ratio is diagnostic for the provenance of the lunar meteorites: High ratios are typical for lunar highlands, low ratios for lunar mare regions. For references see *Lorenzetti et al.* (2005).

events, resulting in craters with diameters of much less than 10 km. The smaller size of these craters relative to those responsible for the ejection of martian meteorites and the regolith structure of the lunar surface may explain why lunar meteorites were generally ejected from <1000 g/cm^2 (<5 m) depth (*Vogt et al.,* 1993b) and often show a complex exposure history.

5. RECORDS OF EARLY PARTICLE RADIATION

Processes of light-element synthesis in solar system materials by SCRs from an active early Sun were suggested by *Fowler et al.* (1962), and recently received renewed attention from the evidence for the presence of short-lived nuclides ^{10}Be, ^{26}Al, ^{36}Cl, ^{41}Ca, and ^{60}Fe in CAIs from primitive chondrites, as well as in chondrules. The evaluation of required particle fluxes and of variations in the isotopic compositions of elements due to decay of these short-lived radionuclides are discussed by *Chaussidon and Gounelle* (2006). These authors also summarize evidence for and estimates of the required fluences to explain the excesses of ^{21}Ne and ^{38}Ar in gas-rich meteorites, as well as recently suggested models for producing non-mass-dependent isotopic anomalies by solar UV radiation.

Solar-mass stars during their early evolution go through a phase of increased activity while en route to the main sequence, and this evolution is characterized by strong stellar winds, increased SCR activity, and increased ultraviolet luminosity. During this phase, particle fluxes would be considerably different from contemporary particle fluxes, and increased activity would have resulted in increased SCR production rates. There is considerable uncertainty about the duration of this phase, and it is not clear when this phase occurred with respect to the formation of the meteorites. If the active phase of the Sun ended prior to the formation of meteorites, then the meteorites themselves would contain no direct evidence for the existence of increased stellar activity. Also, solar nebular gases or solids may have partially or totally blocked this radiation at asteroidal distances. As a result, meteoritic matter may or may not have recorded effects from an enhanced particle flux.

Further complicating the picture is our limited knowledge of the early history of the meteorites and their precursor components that may carry records of the energetic-particle environment. As discussed in this chapter, the much better knowledge of the contemporary energetic particle environment permits calculation of CRE ages. However, these inferred production rates may differ significantly from the rates prevalent in the early solar system. In the introduction we mentioned that precursors of the meteorites may have been exposed during accretion and that other components were probably exposed during regolith processes. *Polnau et al.* (2001) presented evidence for excess amounts of light noble gas spallation components in chondrules, particularly in chondrites with short CRE ages, such as the Sena chondrite. These authors inferred that a precompaction irradiation is the likely source of excess concentrations.

Furthermore, fossil records of solar particle radiations in asteroidal regoliths were observed in gas-rich meteorites. The evidence was discussed in detail by *Caffee et al.* (1988). Specific records of particle radiations were recently also

studied in a variety of meteoritic regolith breccias (*Ferko et al.,* 2002; *Lorenzetti et al.,* 2003; *Mathew and Marti,* 2003).

6. CONCLUSIONS AND OUTLOOK

The presence of peaks in CRE exposure age distributions, taken in conjunction with spectral observations of asteroids and observations of meteorite falls, shows that a few asteroids have produced most of the rocks that fall to Earth. To illustrate this point we note that about 45% of all H chondrites (Fig. 4) have CRE ages between either 6 and 10 m.y. or 30 and 35 m.y. Thus we infer that a maximum of 4000 of the 7000 H chondrites in collections may have come from collisions other than those leading to the two peaks in the CRE age distribution for H chondrites. Although we cannot yet infer with confidence which spectral type of asteroid produced the H chondrites, we know that one possible class of asteroids, the S-type, comprises about 15% of all asteroids with known spectra. The total number of asteroids with radii greater than 1 km in size is about 1,000,000. Thus, even in the exceedingly unlikely event that each known H chondrite originates on a different asteroid, we would have sampled only a small fraction of the total observed population, a compelling reason to explore the asteroid belt.

As was recognized early on, the short CRE ages (<1500 m.y. for irons and <120 m.y. for stones) relative to the 4560-m.y. age of the solar system permit several conclusions: (1) Ongoing processes (collisions in the asteroid belt, breakup of comets) must replenish the meteoroid population. (2) Meteoroid destruction events (collisions, capture by the Sun and planets, and ejection from the solar system) limit CRE ages of meteoroids, otherwise CRE ages would range up to 4.56 G.y. (3) Matter residing in the top few meters of meteorite parent asteroids either exhibits short lifetimes or constitutes a small fraction of the collisional ejecta. (4) The distribution of collisional events shows that mechanical strength (low for aubrites) cannot be the only important factor in limiting CRE ages. Also, subclasses of iron meteorites (IIE) have short CRE ages (Fig. 8).

Meteoroids populate a size range that astronomers cannot observe directly with present-day optical methods; as a result, the CRE ages and the influx of meteoritic matter have been longstanding problems for dynamicists. Dynamical calculations showed that once a meteoroid's orbit is in resonance with Jupiter, the orbital evolution is chaotic (*Wisdom,* 1985) and the transport to Earth follows a chaotic route and implies short (less than 1 m.y.) CRE ages. As discussed in section 4, the calculations show that the Yarkovsky effect delivers asteroidal meteoroids to resonances on timescales consistent with observed CRE ages. This agreement clearly suggests that the Yarkovsky effect is a major mechanism for orbital evolutions of meteoroids.

Ultimately the attempt should be to tie CRE ages to detailed cratering histories of specific parent bodies. Except for the lunar and martian meteorites, the only meteorites for which a parent body has been assigned are the howardites, eucrites, and diogenites. Their probable parent asteroid is Vesta or multikilometer-sized fragments of Vesta with Vesta-consistent orbital elements. Cosmic-ray exposure ages of this group cluster at 22 m.y. and show minor clusters at 36 and 12 m.y. (Fig. 6). Periodicities in the distribution of CRE ages have been suggested, but the evidence is restricted to possible common clusterings at 6, 13, 25, and 36 m.y. Common cluster statistics were interpreted to reflect enhanced collisional activity in the asteroid belt. For a larger number of meteorites (H chondrites, L chondrites, CM and CI chondrites, acapulcoites, and lodranites), CRE ages inform when, but not on which specific bodies, major collisional events took place.

The available data leave many large gaps. Exposure histories of lunar meteorites, for example, reflect only a blurry picture regarding the "when" of the collisions, i.e., the cratering history of the Moon. The Moon's proximity to Earth suggests that more-frequent, smaller collisions produce recoverable meteorites once escape velocities are achieved. Smaller collisions, in turn, favor ejection of near-surface material with a significant irradiation history on the Moon. Unfortunately, pre-irradiation on the Moon makes it more difficult to resolve the extra cosmogenic nuclide signal accumulated during the transit from Moon to Earth. Thus many of the transit times of lunar meteorites, although clearly short, are known only as upper bounds.

It is desirable to follow the arrival of ejecta from a single collisional event over millions of years in order to test models of orbital evolution. The Antarctic meteorites may supply such a source of information, but detailed results will be a long time coming for two reasons. First, this work requires determinations of terrestrial age and CRE age for each meteorite. Second, there is only a handful of meteorites with terrestrial ages of 1 m.y. or more. In this regard, the recent work of *Heck et al.* (2004) represents an intriguing new approach to tracking meteorite influxes over time.

The one-stage exposure history model breaks down in regolith samples. For this reason, in returned samples from the surfaces of other solar system bodies, the calculation of CRE ages for bulk samples must give way to statistical characterization of exposure. In a sample of lunar soil or a meteoritic breccia containing 1000 grains, for example, each one may have a distinct history of exposure. No experimentalist in the foreseeable future can hope to track these stochastic variations in detail. The relevant extractable parameters are nominal times of exposure at various depths, or perhaps rates of vertical turnover; analyses of cosmogenic nuclides supply little information about horizontal motions in a regolith. Possibly micrometeorites may represent standins for sources of material eroded from asteroidal surfaces.

We emphasize that all discussed CRE ages (except for ^{40}K/K ages and revised ^{38}Ar ages of irons) are based on the assumption of a constant CR flux. We have shown that CR fluxes differed from present values in the early solar system environment and during the period from 150 to 700 m.y. before present. As a goal of future research, the variation of the particle environment and of the GCR flux in the "local" region of the Sun during its galactic rotation

needs to be assessed in detail, in particular during its motion in star-forming regions of the galaxy.

Some of today's frontiers of CRE histories lie at the temporal and spatial boundaries of the solar system, in histories of particles of stardust sequestered for 4.5 G.y. in meteorites, and in solar system and extrasolar particles recovered by missions and spacecraft. The study of these and other planetary samples requires improvement in instrumental sensitivity by orders of magnitude.

Acknowledgments. We thank M. Gounelle, R. Michel, K. Welten, and R. Wieler for helpful comments. Technical support was provided by A. Chaoui and K. Bratschi.

REFERENCES

Albrecht A., Schnabel C., Vogt S., Xue S., Herzog G. F., Begemann F., Weber H. W., Middleton R., Fink D., and Klein J. (2000) Light noble gases and cosmogenic radionuclides in Estherville, Budulan, and other mesosiderites: Implications for exposure histories and production rates. *Meteoritics & Planet. Sci., 35,* 975–986.

Anders E. (1964) Origin, age, and composition of meteorites. *Space Sci. Rev., 3,* 583–714.

Arnold J. R. (1965) The origin of meteorites as small bodies. II. The model. *Astrophys. J., 141,* 1536–1547.

Arnold J. R., Honda M., and Lal D. (1961) Record of cosmic-ray intensity in meteorites. *J. Geophys. Res., 66,* 3519–3531.

Artemieva N. A. and Ivanov B. A. (2002) Ejection of martian meteorites — can they fly? (abstract). In *Lunar and Planetary Science XXXIII,* Abstract #1113. Lunar and Planetary Institute, Houston (CD-ROM).

Axford W. I. (1981) Acceleration of cosmic rays by shock waves. *Proceedings of the 17th International Cosmic-Ray Conference, Paris, 12,* 155.

Begemann F. and Schultz L. (1988) The influence of bulk chemical composition on the production rate of cosmogenic nuclides in meteorites (abstract). In *Lunar and Planetary Science XXIX,* pp. 51–52. Lunar and Planetary Institute, Houston.

Begemann F., Vilcsek E., Nyquist L. E., and Signer P. (1970) The exposure history of the Pitts meteorite. *Earth Planet. Sci. Lett., 9,* 317–321.

Begemann F., Weber H. W., Vilcsek E., and Hintenberger H. (1976) Rare gases and ^{36}Cl in stony-iron meteorites: Cosmogenic elemental production rates, exposure ages, diffusion losses, and thermal histories. *Geochim. Cosmochim. Acta, 40,* 353–368.

Bhandari N., Lal D., Rajan R. S., Arnold J. R., Marti K., and Moore C. B. (1980) Atmospheric ablation in meteorites: A study based on cosmic ray tracks and neon isotopes. *Nucl. Tracks, 4,* 213–262.

Bhattacharya S. K., Goswami J. N., Gupta S. K., and Lal D. (1973) Cosmic ray effects induced in a rock exposed on the Moon or in free space: Contrast in patterns for tracks and isotopes. *Moon, 8,* 253–286.

Biermann L. (1951) Kometenschweife und solare Korpuskularstrahlung. *Z. Astrophys., 29,* 274–286.

Biermann L. (1953) Physical processes in comet tails and their relation to solar activity. *Extrait des Mem. Soc. Roy. Sci. Liege Quatr. Ser.,* pp. 291–302.

Binns W. R., Wiedenbeck M. E., Christian E. R., Cummings A. C., George J. S., Israel H. M., Leske R. A., Mewaldt R. A., Stone E. C., Rosenvinge T. T., and Yanasak N. E. (2001) GCR neon isotopic abundances: Comparison with Wolf-Rayet star models and meteorite abundances. In *Solar and Galactic Composition* (R. F. Wimmer-Schweingruber, ed.), pp. 257–262. American Institute of Physics, New York.

Binzel R. P. and Xu S. (1993) Chips off of asteroid 4 Vesta: Evidence for the parent body of basaltic achondrite meteorites. *Science, 260,* 186–191.

Bogard D. D., Nyquist L. E., Bansal B. M., Garrison D. H., Wiesmann H., Herzog G. F., Albrecht A. A., Vogt S., and Klein J. (1995) Neutron-capture ^{36}Cl, ^{41}Ca, ^{36}Ar, and ^{150}Sm in large chondrites: Evidence for high fluences of thermalized neutrons. *J. Geophys. Res., 100,* 9401–9416.

Bottke W. F. (2002) The dynamical evolution of asteroids and meteoroids via Yarkovsky thermal forces (abstract). *Bull. Am. Astron. Soc., 34,* 934.

Bottke W. F., Rubincam D. P., and Burns J. A. (2000) Dynamical evolution of main belt meteoroids: Numerical simulations incorporating planetary perturbations and Yarkovsky thermal forces. *Icarus, 145,* 301–331.

Branham R. L. Jr. (2002) Kinematics of OB stars. *Astrophys. J., 570,* 190–197.

Burbine T. H., McCoy T. J., Meibom A., Gladman B., and Keil K. (2003) Meteoritic parent bodies: Their number and identification. In *Asteroids III* (W. F. Bottke Jr. et al., eds.), pp. 653–667. Univ. of Arizona, Tucson.

Burnett D. S., Lippolt H. J., and Wasserburg G. J. (1966) The relative isotopic abundance of K^{40} in terrestrial and meteoritic samples. *J. Geophys. Res., 71,* 1249–1269.

Caffee M. W. and Nishiizumi K. (1997) Exposure ages of carbonaceous chondrites: II (abstract). *Meteoritics & Planet. Sci., 32,* A26.

Caffee M. W. and Nishiizumi K. (2001) Exposure history of separated phases from the Kapoeta meteorite. *Meteoritics & Planet. Sci., 36,* 429–437.

Caffee M. W., Goswami J. N., Hohenberg C. M., Marti K., and Reedy R. C. (1988) Irradiation records in meteorites. In *Meteorites and the Early Solar System* (J. F. Kerridge and M. S. Matthews, eds), pp. 205–245. Univ. of Arizona, Tucson.

Caffee M. W., Nishiizumi K., Matsumoto Y., Matsuda J., Komura K., and Nakamura N. (2000) Noble gases and cosmogenic radionuclides in Kobe CK meteorite (abstract). *Meteoritics & Planet. Sci., 35,* A37.

Castagnoli G. C. and Lal D. (1980) Solar modulation effects in terrestrial production of carbon 14. *Radiocarbon, 22,* 133–159.

Chapman C. R., Merline W. J., Thomas P. C., Joseph J., Cheng A. F., and Izenberg N. (2002) Impact history of Eros: Craters and boulders. *Icarus, 155,* 104–118.

Chaussidon M. and Gounelle M. (2006) Irradiation processes in the early solar system. In *Meteorites and the Early Solar System II* (D. S. Lauretta and H. Y. McSween Jr., eds.), this volume. Univ. of Arizona, Tucson.

Consolmagno G. J. and Drake M. J. (1977) Composition and evolution of the eucrite parent body: Evidence from rare earth elements. *Geochim. Cosmochim. Acta, 41,* 1271–1282.

Cressy P. J. Jr. (1972) Cosmogenic radionuclides in the Allende and Murchison carbonaceous chondrites. *J. Geophys. Res., 77,* 4905–4911.

De Zeeuw P. T., Hoogerwerf R., De Bruijne J. H. J., Brown A. G. A., and Blaauw A. (1999) A Hipparcos census of the nearby OB associations. *Astronom. J., 117,* 354–399.

Eberhardt P. (1974) A neon-E-rich phase in the Orgueil carbonaceous chondrite. *Earth Planet. Sci. Lett., 24,* 182–187.

Eberhardt P., Geiss J., and Lutz H. (1963) Neutrons in meteorites. In *Earth Science and Meteoritics* (J. Geiss and E. D. Goldberg, eds.), pp. 143–168. North Holland, Amsterdam.

Eberhardt P., Eugster O., and Geiss J. (1965) Radiation ages of aubrites. *J. Geophys. Res., 70,* 4427–4434.

Eberhardt P., Eugster O., Geiss J., and Marti K. (1966) Rare gas measurements in 30 stone meteorites. *Z. Naturforsch., 21A,* 414–426.

Eberhardt P., Geiss J., Graf H., and Schwaller H. (1971) On the origin of excess ^{131}Xe in lunar rocks. *Earth Planet. Sci. Lett., 12,* 260–262.

Eberhardt P., Jungck M. H. A., Meier F. O., and Niederer F. (1979) Presolar grains in Orgueil: Evidence from neon-E. *Astrophys. J. Lett., 234,* L169–L171.

Eugster O. (1988) Cosmic-ray production rates for ^{3}He, ^{21}Ne, ^{38}Ar, ^{83}Kr, and ^{126}Xe in chondrites based on ^{81}Kr-Kr exposure ages. *Geochim. Cosmochim. Acta, 52,* 1649–1662.

Eugster O. (2003) Cosmic-ray exposure ages of meteorites and lunar rocks and their significance. *Chem. Erde/Geochemistry, 63,* 3–30.

Eugster O. and Lorenzetti S. (2005) Cosmic-ray exposure ages of four acapulcoites and two differentiated achondrites and evidence for a two-layer structure of the acapulcoite-lodranite parent asteroid. *Geochim. Cosmochim. Acta, 69,* 2675–2685.

Eugster O. and Michel T. (1995) Common asteroid break-up events of eucrites, diogenites, and howardites and cosmic-ray production rates for noble gases in achondrites. *Geochim. Cosmochim. Acta, 59,* 177–199.

Eugster O., Eberhardt P., and Geiss J. (1967) ^{81}Kr in meteorites and ^{81}Kr radiation ages. *Earth Planet. Sci. Lett., 2,* 77–82.

Eugster O., Tera F., Burnett D. S., and Wasserburg G. J. (1970) Neutron capture effects in Gd from the Norton County meteorite. *Earth Planet. Sci. Lett., 7,* 436–440.

Eugster O., Michel Th., Niedermann S., Wang D., and Yi W. (1993) The record of cosmogenic, radiogenic, fissiogenic, and trapped noble gases in recently recovered Chinese and other chondrites. *Geochim. Cosmochim. Acta, 57,* 1115–1142.

Eugster O., Eberhardt P., Thalmann Ch., and Weigel A. (1998) Neon-E in CM-2 chondrite LEW90500 and collisional history of CM-2 chondrites, Maralinga, and other CK chondrites. *Geochim. Cosmochim. Acta, 62,* 2573–2582.

Eugster O., Busemann H., Lorenzetti S., and Terribilini D. (2002a) Ejection ages from krypton-81–krypton-83 dating and preatmospheric sizes of martian meteorites. *Meteoritics & Planet. Sci., 37,* 1345–1360.

Eugster O., Busemann H., Kurat G., Lorenzetti S., and Varela M. E. (2002b) Characterization of the noble gases and the CRE age of the D'Orbigny angrite (abstract). *Meteoritics & Planet. Sci., 37,* A44.

Farinella P., Vokrouhlicky D., and Hartmann W. K. (1998) Meteorite delivery via Yarkovsky orbital drift. *Icarus, 132,* 378–387.

Ferko T. E., Wang M-S., Hillegonds D. J., Lipschutz M. E., Hutchison R., Franke L., Scherer P., Schultz L., Benoit P. H., Sears D. W. G., Singhvi A. K., and Bhandari N. (2002) The irradiation history of the Ghubara (L5) regolith breccia. *Meteoritics & Planet. Sci., 37,* 311–327.

Fleischer R. L., Price P. B., Walker R. M., and Maurette M. (1967) Origin of fossil charged particle tracks in meteorites. *J. Geophys. Res., 72,* 333–353.

Fleischer R. L., Price P. B., and Walker R. M. (1975) *Nuclear Tracks in Solids: Principles and Applications.* Univ. of California, Berkeley. 705 pp.

Fowler W. A., Greenstein J. L., and Hoyle F. (1962) Nucleosynthesis during the early history of the solar system. *Geophys. J. Roy. Astron. Soc., 6,* 148–220.

Freundel M., Schultz L., and Reedy R. C. (1986) ^{81}Kr-Kr ages of Antarctic meteorites. *Geochim. Cosmochim. Acta, 50,* 2663–2673.

Gilabert E., Lavielle B., Michel R., Leya I., Neumann S., and Hepers U. (2002) Production of krypton and xenon isotopes in thick stony and iron targets isotropically irradiated with 1600 MeV protons. *Meteoritics & Planet. Sci., 37,* 951–976.

Gladman B. J. (1997) Destination: Earth. Martian meteorite delivery. *Icarus, 130,* 228–246.

Gladman B. J., Burns J. A., Duncan M. J., and Levison H. F. (1995) The dynamical evolution of lunar impact ejecta. *Icarus, 118,* 302–321.

Gladman B. J., Burns J. A., Duncan M., Lee P., and Levison H. F. (1996) The exchange of impact ejecta between terrestrial planets. *Science, 271,* 1387–1392.

Goodrich C. A. (1992) Ureilites: A critical review. *Meteoritics, 27,* 327–352.

Goswami J. N., Sinha N., Nishiizumi K., Caffee M. W., Komura K., and Nakamura K. (2001) Cosmogenic records in Kobe (CK4) meteorite: Implications of transport of meteorites from the asteroid belt (abstract). *Meteoritics & Planet. Sci., 36,* A70–A71.

Gounelle M., Shu F. H., Shang H., Glassgold A. E., Rehm K. E., and Lee T. (2001) Extinct radioactivities and protosolar cosmic rays: Self shielding and light elements. *Astrophys. J., 548,* 1051–1070.

Gounelle M., Shu F. H., Shang H., Glassgold A. E., Rehm K. E., and Lee T. (2004) The origin of short-lived radionuclides and early solar system irradiation (abstract). In *Lunar and Planetary Science XXXV*, Abstract #1629. Lunar and Planetary Institute, Houston (CD-ROM).

Graf T. and Marti K. (1994) Collisional records in LL-chondrites. *Meteoritics, 29,* 643–648.

Graf T. and Marti K. (1995) Collisional history of H chondrites. *J. Geophys. Res., 100,* 21247–21263.

Graf T., Baur H., and Signer P. (1990a) A model for the production of cosmogenic nuclides in chondrites. *Geochim. Cosmochim. Acta, 54,* 2521–2534.

Graf T., Signer P., Wieler R., Herpers U., Sarafin R., Vogt S., Fieni Ch., Pellas P., Bonani G., Suter M., and Wölfli W. (1990b) Cosmogenic nuclides and nuclear tracks in the chondrite Knyahinya. *Geochim. Cosmochim. Acta, 54,* 2511–2520.

Graf T., Marti K., Xue S., Herzog G. F., Klein J., Middleton R., Metzler K., Herd R., Brown P., Wacker J. F., Jull A. J. T., Masarik J., Koslowsky V. T., Andrews H. R., Cornett R. J. J., Davies W. G., Greiner B. F., Imahori Y., McKay J. W., Milton G. M., and Milton J. C. D. (1997) Exposure history of the Peekskill (H6) meteorite. *Meteoritics & Planet. Sci., 32,* 25–30.

Graf T., Caffee M. W., Marti K., Nishiizumi K., and Ponganis K. V. (2001) Dating collisional events: ^{36}Cl-^{36}Ar exposure ages of H-chondritic metals. *Icarus, 150,* 181–188.

Heck P. R., Schmitz B., Baur H., Halliday A. N., and Wieler R. (2004) Fast delivery of meteorites to Earth after a major asteroid collision. *Nature, 430,* 323–325.

Herzog G. F. (2003) Cosmic-ray exposure ages of meteorites. In *Treatise on Geochemistry, Vol. 1: Meteorites, Comets, and*

Planets (A. M. Davis, ed.), pp. 347–380. Elsevier, Oxford.

Herzog G. F., Vogt S., Albrecht A., Xue S., Fink D., Klein J., Middleton R., Weber H. W., and Schultz L. (1997) Complex exposure histories for meteorites with "short" exposure ages. *Meteoritics & Planet. Sci., 32,* 413–422.

Heusser G., Ouyang Z., Oehm J., and Yi W. (1996) Aluminum-26, sodium-22 and cobalt-60 in two drill cores and some other samples of the Jilin chondrite. *Meteoritics & Planet. Sci., 31,* 657–665.

Hidaka H., Ebihara M., and Yoneda S. (1999) High fluences of neutrons determined from Sm and Gd isotopic compositions in aubrites. *Earth Planet. Sci. Lett., 173,* 41–51.

Hidaka H., Ebihara M., and Yoneda S. (2000) Isotopic study of neutron capture effects on Sm and Gd in chondrites. *Earth Planet. Sci. Lett., 180,* 29–37.

Hohenberg C. M., Nichols R. H., Olinger C. T., and Goswami J. N. (1990) Cosmogenic neon from individual grains of CM meteorites: Extremely long pre-exposure histories or an enhanced early particle flux. *Geochim. Cosmochim. Acta, 54,* 2133–2140.

Honda M. (1962) Spallation products distributed in a thick iron target bombarded by 3 BeV protons. *J. Geophys. Res., 67,* 4847–4858.

Honda M., Nagai H., Nagao K., and Miura Y. N. (1996) Cosmogenic products in metal phase of the Brenham pallasite (abstract). *Antarctic Meteorites, 21,* 48–50.

Honda M., Caffee M. W., Miura Y. N., Nagai H., Nagao K., and Nishiizumi K. (2002) Cosmogenic nuclides in the Brenham pallasite. *Meteoritics & Planet. Sci., 37,* 1711–1728.

Hörz F., Grieve R., Heiken G., Spudis P., and Binder A. (1991) Lunar surface processes. In *Lunar Sourcebook: A User's Guide to the Moon* (G. Heiken et al., eds.), pp. 61–120. Cambridge Univ., Cambridge.

Kaiser W. A. and Rajan R. S. (1973) The variation of cosmogenic Kr and Xe in a core from Esterville mesosiderite: Direct evidence that the lunar ^{131}Xe anomaly is a depth effect. *Earth Planet. Sci. Lett., 20,* 286–294.

Kalinina G. V., Kashkarov L. L., Ivleiv A. I., and Skripnik A. Y. (2004) Radiation and shock thermal history of the Kaidun CR2 chondrite glass inclusions (abstract). In *Lunar and Planetary Science XXXV,* Abstract #1075. Lunar and Planetary Institute, Houston (CD-ROM).

Keil K., Haack H., and Scott E. R. D. (1994) Catastrophic fragmentation of asteroids: Evidence from meteorites. *Planet. Space Sci., 42,* 1109–1122.

Kohman T. P. and Bender M. L. (1967) Nuclide production by cosmic rays in meteorites and on the moon. In *High-Energy Reactions in Astrophysics* (B. S. P. Shen, ed.), pp. 169–245. Benjamin, New York.

Lal D. (1972) Hard rock cosmic ray archaeology. *Space Sci. Rev., 14,* 3–102.

Lavielle B., Marti K., and Regnier S. (1985) Ages d'exposition des meteorites de fer: Histoires multiples et variations d'intensité du rayonnement cosmique. In *Isotopic Ratios in the Solar System,* pp. 15–20. Cepadeus-Editions, Toulouse, France.

Lavielle B., Marti K., Jeannot J.-P., Nishiizumi K., and Caffee M. (1999) The ^{36}Cl-^{36}Ar-^{40}K-^{41}K records and cosmic ray production rates in iron meteorites. *Earth Planet. Sci. Lett., 170,* 93–104.

Lavielle B., Caffee M., Gilabert E., Marti K., Nishiizumi K., and Ponganis K. (2001) Irradiation records in group IVA irons. *Meteoritics & Planet. Sci., 36,* A110–A111.

Leya I. and Michel R. (1998) Determination of neutron cross sections for nuclide production at intermediate energies by deconvolution of thick-target production rates. In *Proceedings of the International Conference on Nuclear Data for Science and Technology* (G. Reffo, ed.), pp. 1463–1467. Trieste, Italy.

Leya I., Lange H.-J., Neumann S., Wieler R., and Michel R. (2000) The production of cosmogenic nuclides in stony meteoroids by galactic cosmic ray particles. *Meteoritics & Planet. Sci., 35,* 259–286.

Leya I., Wieler R., Aggrey K., Herzog G. F., Schnabel C., Metzler K., Hildebrand A. R., Bouchard M., Jull A. J. T., Andrews H. R., Wang M.-S., Ferko T. E., Lipschutz M. E., Wacker J. F., Neumann S., and Michel R. (2001a) Exposure history of the St-Robert (H5) fall. *Meteoritics & Planet. Sci., 36,* 1479–1494.

Leya I., Graf T., Nishiizumi K., and Wieler R. (2001b) Cosmic-ray production rates of He-, Ne-, and Ar-isotopes in H-chondrites based on ^{36}Cl-^{36}Ar ages. *Meteoritics & Planet. Sci., 36,* 963–973.

Leya I., Halliday A., and Wieler R. (2003) The predictable collateral consequences of nucleosynthesis by spallation reactions in the early solar system. *Astrophys. J., 594,* 605–616.

Leya I., Begemann F., Weber H. W., Wieler R., and Michel R. (2004a) Simulation of the interaction of galactic cosmic ray protons with meteoroids: On the production of ^{3}H and light noble gas isotopes in isotropically irradiated thick gabbro and iron targets. *Meteoritics & Planet. Sci., 39,* 367–386.

Leya I., Gilabert E., Lavielle B.,Wiechert U., and Wieler R. (2004b) Production rates for cosmogenic krypton and argon isotopes in H-chondrites with known ^{36}Cl-^{36}Ar ages. *Antarct. Met. Res., 17,* 185–199.

Lingenfelter R. E., Canfield E. H., and Hampel V. E. (1972) The lunar neutron flux revisited. *Earth Planet. Sci. Lett., 16,* 355–369.

Lingenfelter R. E., Higdon J. C., and Ramaty R. (2000) Cosmic ray acceleration in superbubbles and the compositon of cosmic rays. In *Acceleration and Transport of Energetic Particles Observed in the Heliosphere* (R. Mewaldt et al., eds.), pp. 375. American Institute of Physics, New York.

Lorenzetti S., Eugster O., Busemann H., Marti K., Burbine T. H., and McCoy T. (2003) History and origin of aubrites. *Geochim. Cosmochim. Acta, 67,* 557–571.

Lorenzetti S., Busemann H., and Eugster O. (2005) Regolith history of lunar meteorites. *Meteoritics & Planet. Sci., 40,* 315–327.

Lüpke M. (1993) Untersuchungen zur Wechselwirkung galaktischer Protonen mit Meteoroiden-Dicktarget Simulationsexperimenten und Messung von Dünntarget-Wirkungsquerschnitten. Ph.D. thesis, University of Hannover, Germany.

Marti K. (1967) Mass-spectrometric detection of cosmic-ray-produced Kr^{81} in meteorites and the possibility of Kr-Kr dating. *Phys. Rev. Lett., 18,* 264–266.

Marti K. (1986) Live ^{129}I-^{129}Xe dating. In *Workshop on Cosmogenic Nuclides* (R. C. Reedy and P. Englert, eds.), pp. 49–51. LPI Tech. Rpt. 86-06, Lunar and Planetary Institute, Houston.

Marti K. and Graf T. (1992) Cosmic-ray exposure history of ordinary chondrites. *Annu. Rev. Earth Planet. Sci., 20,* 221–243.

Marti K. and Lugmair G. W. (1971) Kr^{81}-Kr and K-Ar^{40} ages, cosmic-ray spallation products, and neutron effects in lunar samples from Oceanus Procellarum. *Proc. Lunar. Sci. Conf. 2nd,* pp. 1591–1605.

Marti K., Eberhardt P., and Geiss J. (1966) Spallation, fission, and neutron capture anomalies in meteoritic krypton and xenon.

Z. Naturforsch., 21a, 398–413.

Marti K., Lingenfelter R., Mathew K. J., and Nishiizumi K. (2004) Cosmic rays in the solar neighborhood (abstract). *Meteoritics & Planet. Sci., 39,* A63.

Masarik J. and Reedy R. C. (1994) Effects of bulk composition on nuclide production processes in meteorites. *Geochim. Cosmochim. Acta, 58,* 5307–5317.

Masarik J., Nishiizumi K., and Reedy R. C. (2001) Production rates of ^{3}He, ^{21}Ne, and ^{22}Ne in ordinary chondrites and the lunar surface. *Meteoritics & Planet. Sci., 36,* 643–650.

Mathew K. J. and Marti K. (2003) Solar wind and other gases in the regoliths of the Pesyanoe parent object and the moon. *Meteoritics & Planet. Sci., 38,* 627–643.

McCoy T. J., Keil K., Clayton R. N., Mayeda T. K., Bogard D. D., Garrison D. H., Wieler R. (1997) A petrologic and isotopic study of lodranites: Evidence for early formation as partial melt residues from heterogeneous precursors. *Geochim. Cosmochim. Acta, 61,* 623–637.

Megrue G. H. (1968) Rare gas chronology of hypersthene achondrites and pallasites. *J. Geophys. Res., 73,* 2027–2033.

Meyer C. (2003) *Mars Meteorite Compendium-2003, Revision B.* JSC Publ. No. 27672, NASA Johnson Space Center, Houston.

Michel R., Dragovitsch P., Englert P., Peiffer F., Stuck R., Theis S., Begemann F., Weber H., Signer P., Wieler R., Filges D., and Cloth P. (1986) On the depth dependence of spallation reactions in a spherical thick diorite target homogeneously irradiated by 600 MeV protons: Simulation of production of cosmogenic nuclides in small meteorites. *Nucl. Instrum. Methods, B16,* 61–82.

Michel R., Dragovitsch P., Cloth P., Dagge G., and Filges D. (1991) On the production of cosmogenic nuclides in meteoroids by galactic protons. *Meteoritics, 26,* 221–242.

Michel R., Lüpke M., Herpers U., Rösel R., Suter M., Dittrich-Hannen B., Kubik P. W., Filges D., and Cloth P. (1995) Simulation and modelling of the interaction of galactic protons with stony meteoroids. *Planet. Space Sci., 43,* 557–572.

Michel R., Leya I., and Borges L. (1996) Production of cosmogenic nuclides in meteoroids — Accelerator experiments and model calculations to decipher the cosmic ray record in extraterrestrial matter. *Nucl. Instrum. Methods Phys. Res., B113,* 434–444.

Miura Y. N. (1995) Studies on differentiated meteorites: Evidence from ^{244}Pu-derived fission Xe, ^{81}Kr, other noble gases and nitrogen. Ph.D. thesis, Univ. of Tokyo. 212 pp.

Miura Y. N., Nagao K., Sugiura N., Fujitani T., and Warren P. H. (1998) Noble gases ^{81}Kr-Kr exposure ages and ^{244}Pu-Xe ages of six eucrites, Béréba, Binda, Camel Donga, Juvinas, Millbillillie, and Stannern. *Geochim. Cosmochim. Acta, 62,* 2369–2387.

Nishiizumi K. and Caffee M. W. (2002) Exposure histories of C2 carbonaceous chondrites (abstract). *Meteoritics & Planet. Sci., 37,* A109.

Nishiizumi K., Regnier S., and Marti K. (1980) Cosmic ray exposure ages of chondrites, pre-irradiation and constancy of cosmic ray flux in the past. *Earth Planet. Sci. Lett., 50,* 150–170.

Nishiizumi K., Arnold J. R., Caffee M. W., Finkel R. C., Southon J. R., Nagai H., Honda M., Imamura M., Kobayashi K., and Sharma P. (1993a) Exposure ages of carbonaceous chondrites (abstract). In *Lunar and Planetary Science XXIV,* pp. 1085–1086. Lunar and Planetary Institute, Houston.

Nishiizumi K., Arnold J. R., and Sharma P. (1993b) Two-stage exposure of the Fayetteville meteorite based on ^{129}I (abstract). *Meteoritics, 28,* 412.

Nishiizumi K., Caffee M. W., Bogard D. D., Garrison D. H., and Kyte F. T. (2000) Noble gases and cosmogenic radionuclides in the Eltanin meteorite (abstract). In *Lunar and Planetary Science XXXI,* Abstract #2070. Lunar and Planetary Institute, Houston (CD-ROM).

Nyquist L. E., Funk H., Schultz L., and Signer P. (1973) He, Ne, and Ar in chondritic Ni-Fe as irradiation hardness sensors. *Geochim. Cosmochim. Acta, 37,* 1655–1685.

Nyquist L. E., Bogard D. D., Shih C.-Y., Greshake A., Stöffler D., and Eugster O. (2001) Ages and geologic histories of martian meteorites. *Space Sci. Rev., 96,* 105–164.

Okazaki R., Takaoka N., Nakamura T., and Nagao K. (2000) Cosmic-ray exposure ages of enstatite chondrites. *Antarct. Meteorite Res., 13,* 153–169.

Ott U. and Begemann F. (2000) Spallation recoil and age of presolar grains in meteorites. *Meteoritics & Planet. Sci., 35,* 53–63.

Ott U., Löhr H.-P., and Begemann F. (1985) Noble gases and the classification of Brachina. *Meteoritics, 20,* 69–78.

Ott U., Löhr H. P., and Begemann F. (1987) Noble gases in ALH 84025: Like Brachina, unlike Chassigny. *Meteoritics, 22,* 476–477.

Padia J. T. and Rao M. N. (1989) Neon isotope studies of Fayetteville and Kapoeta meteorites and clue to ancient solar activity. *Geochim. Cosmochim. Acta, 53,* 1461–1467.

Patzer A. and Schultz L. (2001) Noble gases in enstatite chondrites I: Exposure ages, pairing, and weathering effects. *Meteoritics & Planet. Sci., 36,* 947–961.

Patzer A., Schultz L., and Francke L. (2003) New noble gas data of primitive and differentiated achondrites including NWA 011 and Tafassasset. *Meteoritics & Planet. Sci., 38,* 1485–1498.

Pepin R. O., Palma R. L., and Schlutter D. J. (2001) Noble gases in interplanetary dust particles, II: Excess helium-3 in cluster particles and modeling constraints on interplanetary dust particle exposures to cosmic-ray irradiation. *Meteoritics & Planet. Sci., 36,* 1515–1534.

Polnau E., Eugster O., Burger M., Krähenbühl U., and Marti K. (2001) The precompaction exposure of chondrules and implications. *Geochim. Cosmochim. Acta, 65,* 1849–1866.

Pomerantz M. A. and Duggal S. P. (1974) The Sun and cosmic rays. *Rev. Geophys. Space Phys., 12,* 343–361.

Ramaty R., Kozlovsky B., and Lingenfelter R. E. (1996) Light isotopes, extinct radioisotopes, and gamma-ray lines from low-energy cosmic-ray interactions. *Astrophys. J., 456,* 525–540.

Rao M. N., Garrison D. H., Palma R. L., and Bogard D. D. (1997) Energetic proton irradiation history of the howardite parent body regolith and implications for ancient solar activity. *Meteoritics & Planet. Sci., 32,* 531–543.

Reedy R. C. (1985) A model for GCR-particle fluxes in stony meteorites and production rates of cosmogenic nuclides. *Proc. Lunar Planet. Sci. Conf. 15th,* in *J. Geophys. Res., 90,* C722–C728.

Reedy R. C. (1987) Predicting the production rates of cosmogenic nuclides in extraterrestrial matter. *Nucl. Instrum. Meth., B29,* 251–261.

Reedy R., Arnold J. R., and Lal D. (1983) Cosmic-ray record in solar system matter. *Science, 219,* 127–135.

Reeves H. (1978) Supernovae contamination of the early solar system in an OB stellar association or the "Bing Bang" theory of the origin of the solar system. In *Protostars and Planets* (T. Gehrels, ed.), pp. 399–426. Univ. of Arizona, Tucson.

Rubin A., Kallemeyn G. W., Wasson J. T., Clayton R. N., Mayeda T. K., Grady M., Verchovsky A. B., Eugster O., Lorenzetti S. (2003) Formation of metal and silicate globules in Gujba: A new Bencubbin-like meteorite fall from Nigeria. *Geochim. Cosmochim. Acta, 67,* 3283–3298.

Schaeffer O. A., Nagel K., Fechtig H., and Neukum G. (1981) Space erosion of meteorites and the secular variation of cosmic rays (over 10^9 years). *Planet. Space Sci., 29,* 1109–1118.

Scherer P. and Schultz L. (2000) Noble gas record, collisional history, and paring of CV, CO, CK, and other carbonaceous chondrites. *Meteoritics & Planet. Sci., 35,* 145–153.

Scherer P., Zipfel J., and Schultz L. (1998) Noble gases in two new ureilites from the Saharan desert (abstract). In *Lunar and Planetary Science XXIX,* Abstract #1383. Lunar and Planetary Institute, Houston (CD-ROM).

Schnabel C., Herzog G. F., Pierazzo E., Xu S., Masarik J., Cresswell R. G., di Tada M. L., Liu K., and Fifield L. K. (1999) Shock melting of the Canyon Diablo impactor: Constraints from nickel-59 and numerical modeling. *Science, 285,* 85–88.

Schnabel C., Ma P., Herzog G. F., Faestermann T., Knie K., and Korschinek G. (2001) ^{10}Be, ^{26}Al, and ^{53}Mn in martian meteorites (abstract). In *Lunar and Planetary Science XXXII,* Abstract #1353. Lunar and Planetary Institute, Houston (CD-ROM).

Schnabel C., Leya I., Gloris M., Michel R., Lopez-Gutirérrez J. M., Krähenbühl U., Herpers U., Kuhnhenn J., and Synal H. A. (2004) Production rates and proton-induced production of cross sections of ^{129}I from Te and Ba. An attempt to model the ^{129}I production in stony meteoroids and ^{129}I in a Knyahinya sample. *Meteoritics & Planet. Sci., 39,* 453–466.

Schultz L. and Franke L. (2004) Helium, neon, and argon in meteorites: A data collection. *Meteoritics & Planet. Sci., 39,* 1889–1890.

Schultz L. and Signer P. (1977) Noble gases in the St. Mesmin chondrite: Implications to the irradiation history of a brecciated meteorite. *Earth Planet. Sci. Lett., 36,* 363–371.

Schultz L., Signer P., Lorin J. C., and Pellas P. (1972) Complex irradiation history of the Weston chondrite. *Earth Planet. Sci. Lett., 15,* 403–410.

Schultz L., Weber H. W., and Franke L. (2005) Rumuruti (R)-chondrites: Noble gases, exposure ages, pairing and parent body history. *Meteoritics & Planet. Sci., 40,* 557–571.

Shukolyukov Y. A. and Begemann F. (1996) Cosmogenic and fissiogenic noble gases and ^{81}Kr-Kr exposure age clusters of eucrites. *Meteoritics & Planet. Sci., 31,* 60–72.

Shukolyukov Y. A. and Petaev M. I. (1992) Noble gases in the Omolon pallasite (abstract). In *Lunar and Planetary Science XXIII,* pp. 1297–1298. Lunar and Planetary Institute, Houston.

Spergel M. S., Reedy R. C., Lazareth O. W., Levy P. W., and Slates L. A. (1986) Cosmogenic neutron-capture-produced nuclides in stony meteorites. *Proc. Lunar Planet. Sci. Conf. 16th,* in *J. Geophys. Res., 91,* D483–D494.

Spitale J. and Greenberg R. (2002) Numerical evaluation of the general Yarkovsky effect: Effects on eccentricity and longitude of periapse. *Icarus, 156,* 211–222.

Stauffer H. (1962) On the production ratios of rare gas isotopes in stone meteorites. *J. Geophys. Res., 67,* 2023–2028.

Swindle T. D., Kring D. A., Burkland M. K., Hill D. H., and Boynton W. F. (1998) Noble gases, bulk chemistry, and petrography of olivine-rich achondrites Eagles Nest and Lewis Cliff 88763: Comparison to brachinites. *Meteoritics & Planet. Sci., 33,* 31–48.

Terribilini D., Eugster O., Herzog G. F., and Schnabel C. (2000a) Evidence for common break-up events of the acapulcoites/lodranites and chondrites. *Meteoritics & Planet. Sci., 35,* 1043–1050.

Terribilini D., Eugster O., Mittlefehldt D. W., Diamond L. W., Vogt S., and Wang D. (2000b) Mineralogical and chemical composition and cosmic-ray exposure history of two mesosiderites and two iron meteorites. *Meteoritics & Planet. Sci., 35,* 617–628.

Ustinova G. K. (2002) Mechanisms of isotopic heterogeneity generation by shock waves in the primary matter of the solar system. *Geochem. Intl., 40,* 827–842.

Vogt S., Herzog G. F., and Reedy R. C. (1990) Cosmogenic nuclides in extraterrestrial materials. *Rev. Geophys., 28,* 253–275.

Vogt S., Aylmer D., Herzog G. F., Wieler R., Signer P., Pellas P., Fiéni C., Tuniz C., Jull A. J. T., Fink D., Klein J., and Middleton R. (1993a) Multi-stage exposure history of the H5 chondrite Bur Gheluai. *Meteoritics, 28,* 71–85.

Vogt S. K., Herzog G. F., Eugster O., Michel Th., Niedermann S., Krähenbühl U., Middleton R., Dezfouly-Arjomandy B., Fink D., and Klein J. (1993b) Exposure history of the lunar meteorite Elephant Moraine 87521. *Geochim. Cosmochim. Acta, 57,* 3793–3799.

Voshage H. (1967) Bestrahlungsalter und Herkunft der Eisenmeteorite. *Z. Naturforsch., 22a,* 477–506.

Voshage H. (1982) Investigations of cosmic-ray-produced nuclides in iron meteorites, 4. Identification of noble gas abundance anomalies. *Earth Planet. Sci. Lett., 61,* 32–40.

Voshage H. and Feldmann H. (1979) Investigations of cosmic-ray-produced nuclides in iron meteorites, 3: Exposure ages, meteoroid sizes and sample depths determined by spectrometric analyses of potassium and rare gases. *Earth Planet. Sci. Lett., 45,* 293–308.

Voshage H. and Hintenberger H. (1963) The cosmic-ray exposure ages of iron meteorites as derived from the isotopic composition of potassium and the production rates of cosmogenic nuclides in the past. In *Radioactive Dating,* pp. 367–379. International Atomic Energy Agency, Vienna.

Voshage H., Feldmann H., and Braun O. (1983) Investigations of cosmic-ray-produced nuclides in iron meteorites: 5. More data on the nuclides of potassium and noble gases, on exposure ages and meteoroid sizes. *Z. Naturforsch., 38a,* 273–280.

Vokrouhlicky D., Milani A., and Chesley S. R. (2000) Yarkovsky effect on small near-Earth asteroids: Mathematical formulation and examples. *Icarus, 148,* 118–138.

Warren P. H. (1994) Lunar and Martian meteorite delivery services. *Icarus, 111,* 338–363.

Weigel A., Eugster O., Koeberl C., Michel R., Krähenbühl U., and Neumann S. (1999) Relationships among lodranites and acapulcoites: Noble gas isotopic abundances, chemical composition, cosmic-ray exposure ages, and solar cosmic ray effects. *Geochim. Cosmochim. Acta, 63,* 175–192.

Welten K. C., Lindner L., van der Berg K., Loeken T., Scherer P., and Schultz L. (1997) Cosmic-ray exposure ages of diogenites and the recent collisional history of the howardite, eucrite and diogenite parent body/bodies. *Meteoritics & Planet. Sci., 32,* 891–902.

Welten K. C., Nishiizumi K., Caffee M. W., and Schultz L. (2001a) Update on exposure ages of diogenites: The impact history of the HED parent body and evidence of space erosion and/or collisional disruption of stony meteoroids (abstract). *Meteoritics & Planet. Sci., 36,* A223.

Welten K. C., Bland P. A., Russell S. S., Grady M. M., Caffee

M. W., Masarik J., Jull A. J. T., Weber H. W., and Schultz L. (2001b) Exposure age and pre-atmospheric radius of the Chinguetti-mesosiderite: Not part of a much larger mass. *Meteoritics & Planet. Sci., 36,* 939–946.

Welten K. C., Caffee M. W., Leya I., Masarik J., Nishiizumi K., and Wieler R. (2003) Noble gases and cosmogenic radionuclides in the Gold Basin L4-chondrite shower: Thermal history, exposure history, and pre-atmospheric size. *Meteoritics & Planet. Sci., 38,* 157–174.

Welten K., Nishiizumi K., Caffee M. W., Hillegonds D. J., Leya I., Wieler R., and Masarik J. (2004) The complex exposure history of a very large L/LL5 chondrite shower: Queen Alexandra Range 90201 (abstract). In *Lunar and Planetary Science XXXV,* Abstract #2020. Lunar and Planetary Institute, Houston (CD-ROM).

Wieler R. (2002a) Cosmic-ray-produced noble gases in meteorites. *Rev. Mineral. Geochem., 47,* 125–170.

Wieler R. (2002b) Noble gases in the solar system. *Rev. Mineral. Geochem., 47,* 21–70.

Wieler R. and Graf T. (2001) Cosmic ray exposure history of meteorites. In *Accretion of Extraterrestrial Material Throughout Earth's History* (B. Peucker-Ehrenbrink and B. Schmitz, eds.), pp. 221–240. Kluwer Academic/Plenum, New York.

Wieler R., Graf T., Pedroni A., Signer P., Pellas P., Fieni C., Suter M., Vogt S., Clayton R. N., and Laul J. C. (1989) Exposure history of the regolithic chondrite Fayetteville: II. Solar-gas-free light inclusions. *Geochim. Cosmochim. Acta, 53,* 1449–1459.

Wieler R., Graf T., Signer P., Vogt S., Herzog G. F., Tuniz C., Fink D., Fifield L. K., Klein J., Middleton R., Jull A. J. T., Pellas P., Masarik J., and Dreibus G. (1996) Exposure history of the Torino meteorite. *Meteoritics & Planet. Sci., 31,* 265–272.

Wieler R., Pedroni A., and Leya I. (2000) Cosmogenic neon in mineral separates from Kapoeta: No evidence for an irradiation of its parent body regolith by an early active Sun. *Meteoritics & Planet. Sci., 35,* 251–257.

Wieler R., Busemann H., and Franchi I. A. (2006) Trapping and modification processes of noble gases and nitrogen in meteorites and their parent bodies. In *Meteorites and the Early Solar System II* (D. S. Lauretta and H. Y. McSween Jr., eds.), this volume. Univ. of Arizona, Tucson.

Wisdom J. (1985) A perturbative treatment of motion near 3:1 commensurability. *Icarus, 63,* 272–289.